NetShaper: A Differentially Private Network Side-Channel Mitigation System

Paper # 168

Abstract

The widespread adoption of encryption in network protocols has significantly improved the overall security of many Internet applications. However, these protocols cannot prevent *network side-channel leaks*—leaks of sensitive information through the sizes and timing of network packets. We present NetShaper, a system that mitigates such leaks based on the principle of traffic shaping. NetShaper's traffic shaping provides differential privacy guarantees while adapting to the prevailing workload and congestion condition, and allows configuring a tradeoff between privacy guarantees, bandwidth and latency overheads. Furthermore, NetShaper provides a modular and portable tunnel endpoint design that can support diverse applications. We present a middlebox-based implementation of NetShaper and demonstrate its applicability in a video streaming and a web service application.

1 Introduction

With the proliferation of TLS and VPN, traffic encryption has become the de facto standard for securing data in transit in Internet applications. Traffic can be encrypted at various layers, such as HTTPS, QUIC, and IPSec. While these protocols prevent *direct* data breaches on the Internet, they cannot prevent leaks through *indirect* observations of the encrypted traffic.

Indeed, encryption cannot conceal the shape of an application's traffic, i.e., the sizes, timing, and number of packets sent and received by an application. In many applications, these parameters strongly correlate with sensitive information. For instance, traffic shape can reveal video streams [61], website visits [15, 74], the content of VoIP conversations [77], and even users' medical and financial secrets [20].

In such *network side-channel leaks*, an adversary (e.g., a malicious or a compromised ISP) observes the shape of an application's traffic as it passes through a link under its control and infers the application's sensitive data from this shape.

Obfuscation techniques, which add ad hoc noise [48] or adversarial noise [6, 33, 38, 53, 57, 62] in an application's network traces, do not provide comprehensive protection against network side-channel attacks [82]. In fact, recent advances in machine learning (ML) have greatly improved the ability to filter out noise due to congestion or path variations and infer secrets from noisy data [15, 34, 61, 65]. For instance, our own novel classifier ~~, which is~~ based on Temporal Convolution Networks (TCN) [10] ~~,~~ can infer video streams even from short bursts of noisy measurements over the Internet (see §2 for details). Alternatively, a sensitive application could try to improve side-channel resilience by splitting traffic over multiple network paths [24, 73] or by using dedicated physical links that are not controlled by the adversary. However, such solutions are inadequate against a powerful adversary that can monitor a large fraction of the Internet [14] and may incur prohibitive network administration costs for small users on the Internet.

In contrast, a principled and practical approach to mitigating network side-channel leaks is *traffic shaping*. It involves modifying the victim's packet sizes and timing to make the resultant shape independent of secrets, so that an adversary cannot infer the secrets despite observing the (shaped) traffic.

Constant shaping involves sending fixed-sized packets at a constant rate, which is secure but incurs non-trivial bandwidth and/or latency overhead for applications with variable or bursty workloads [60]. Variable shaping strategies attempt to adapt traffic shapes to reduce the overhead at the cost of some privacy. However, the state-of-the-art (SOTA) variable shaping strategies rely on ad hoc heuristics that yield weak privacy guarantees [55, 74, 75] or unbounded privacy leaks [17, 18, 32, 40, 47]. Some techniques provide strong guarantees but require extensive a priori profiling of an applications' traffic to compute shapes [49, 82].

In addition to a shaping strategy, network side-channel mitigation also requires a robust implementation of packet padding and transmit scheduling. Many solutions attempt to protect traffic by controlling shaping from only one end of a communication (i.e., either a client or a server) and provide only best-effort protection [21, 48, 66]. Other solutions rely on trusting third-party mediators (e.g., Tor bridges), which implement shaping between the clients and mediators and between

the servers and mediators [52, 78]. In Pacer [49], both application endpoints integrate a shaping system to comprehensively mitigate network side channels. However, Pacer encumbers application end hosts with non-trivial changes in the network stack to implement shaping, thus deterring adoption.

In this work, we address two main questions. First, is there ~~an adaptive~~ a variable traffic shaping strategy that provides quantifiable and tunable privacy guarantees at runtime without requiring extensive pre-profiling of application traffic? Second, can traffic shaping be provided as a generic, portable, and efficient solution that can be integrated in different network settings and can support diverse applications?

We present NetShaper, a network side-channel mitigation system that answers both questions in the affirmative. First, NetShaper relies on a differential privacy (DP) based traffic shaping strategy, which provides quantifiable and tunable privacy guarantees. NetShaper specifies ~~DP~~ the privacy parameters for a configurable window of transmission. Moreover, it can configure the parameters independently for each direction of traffic on a communication link. The DP guarantees can be composed based on these parameters to achieve bounded privacy leaks for arbitrary bidirectional traffic. Overall, applications can tune the shaping based only on the privacy guarantees they desire and the overheads they can afford, ~~and~~ without the need for profiling their traffic. While strong privacy guarantees require DP parameters that incur large overheads, in practice, NetShaper can defeat SOTA attacks with even small amounts of DP noise, thus incurring low overheads.

Secondly, we present a traffic shaping tunnel with a modular endpoint design that can conceptually be integrated with any network stack and within any node. The tunnel implements padding and transmit scheduling of packets while adhering to the DP guarantees *by design*. By placing the tunnel endpoint in a middlebox at the edge of the private network, NetShaper can simultaneously protect the traffic of multiple applications. Moreover, the middlebox can amortize the shaping overheads among multiple flows without compromising the privacy for individual flows.

Together, the DP shaping strategy and NetShaper's tunnel provide effective network side-channel mitigation for diverse applications, such as video streaming and web services, with modest overheads. To the best of our knowledge, NetShaper is the first system to provide dynamic traffic shaping with quantifiable and tunable privacy guarantees based on DP.

~~**Contributions.**~~ **Contributions.** (i) We design a new attack classifier based on a Temporal Convolution Network (TCN) [10] and demonstrate its ability to infer videos streams from traffic shapes under noisy network traffic measurements in the Internet (§2). (ii) We model network side-channel mitigations as a differential privacy problem and provide a traffic shaping strategy that offers (ε,δ)-differential privacy guarantees (§3). (iii) We design a QUIC-based traffic shaping tunnel and present a middlebox-based implementation of the tunnel, which supports traffic shaping while adhering to DP guarantees (§4). (iv) We demonstrate NetShaper's efficacy in defeating a SOTA classifier [61] and our new TCN classifier. We empirically evaluate the tradeoffs between NetShaper's privacy guarantees and performance overheads while mitigating network side-channel leaks in two classes of applications that have already been used in prior work, namely video streaming and web service (§5). (vi) We present a formal proof of NetShaper's differential privacy guarantees (§B).

2 Background, Motivation, and Overview

2.1 Network Side-Channel Attacks

We start by explaining the workings of a network side-channel attack with an example application. Consider MedFlix, a fictitious medical video service that offers videos on symptoms, treatment procedures, and post-operative care. ~~We demonstrate an example network side-channelattack. The goal~~ The goal of an adversary is to infer ~~from the traffic shape the videos being~~ the videos streamed by users visiting the service. ISPs can aggregate such information to build per-user profiles and subsequently monetize them. Additionally, competitors might exploit network side channels to acquire corporate intelligence without detection.

~~We set up the~~ The adversary performs the attack in two stages. First, the adversary requests each video from the medical service as a client and collects traces of the bidirectional network traffic generated while streaming each video. The adversary may collect multiple traces for each video stream to account for network variations in the traffic. The adversary then builds a classifier over the captured traces to identify the video streams. Prior work has used several features for classification, such as packet sizes, inter-packet timing, total bytes transferred in a burst of packets, the burst duration and inter-burst interval, and the direction of packets or bursts [61].

We reproduce the Beauty and the Burst (BB) classifier [61], a state-of-the-art CNN classifier for classifying video streams from network traces. Furthermore, we present a new TCN classifier [10], which is an improvement over the BB classifier. We describe the classifiers in §A. Here, we evaluate the efficacy of the two classifiers for a network side-channel attack.

We set up a video service and a video client as two Amazon AWS VMs placed in Oregon and Montreal, respectively. The video server hosts a dataset of 100 YouTube videos at 720p resolution with MPEG-DASH encoding [76]. The client streams the first 5 min of each video over HTTPS and collects the resulting network packet traces using tcpdump. We stream each video 100 times, thus collecting a total of 10,000 traces.

~~We reproduce Beauty and the Burst (BB) , a SOTA CNN classifier. We also present a new TCN classifier , which is~~

~~robust to noisy measurements over the Internet.~~ The classifiers' goal is to predict the video from a network trace. ~~(We describe the classifiers in §A.)~~ For each classifier, we transform each packet trace into a sequence of burst sizes transmitted within 1s windows and normalize the sequence by dividing each burst size by the total size of all bursts. We evaluate the performance of both classifiers with ~~two~~ three datasets: a small dataset consisting of ~~40 videos with~~ 20 videos with their 100 traces each (i.e., total 2000 traces), a medium dataset with 40 videos (4000 traces), and a large dataset comprising all ~~100 videos (10000~~ 100 videos (10000 traces). We train the classifiers for 1000 epochs with an 80-20 train-test split. BB's classification accuracy, recall, and precision with the small dataset are ~~,respectively, but all drop to with the~~ 0.85, 0.85, and 0.78, respectively, which drop to 0.61, 0.63, and 0.49, respectively, with the medium dataset, and further drop to 0.01 each for the large dataset. TCN's accuracy, recall, and precision are ~~all above for both datasets.~~above 0.99 for all datasets. TCN performs better than BB because it is a complex model with residual layers and, hence, is robust to noise in the traces.

Similarly, advanced ML classifiers are capable of identifying web traffic [15, 65]. In general, classifiers will continue to evolve, increasing the adversary's capabilities to make inferences from noisy measurements. Hence, we need principled mitigations that address current SOTA attacks and achieve quantifiable leakage, which can be configured based on privacy requirements and overhead tolerance.

2.2 Key Ideas

A secure and practical network side-channel mitigation system must satisfy the following design goals: **G1.** Mitigate leaks through all aspects of the shape of transmitted traffic, **G2.** Provide quantifiable and tunable privacy guarantees for the communication parties, **G3.** Minimize overheads incurred while guaranteeing privacy, **G4.** Support a broad class of applications, and **G5.** Require minimal changes to applications.

NetShaper's shaping prevents leaks of the traffic content through sizes and timing of packets transmitted along each direction between application nodes (G1). In addition, NetShaper relies on the following three key ideas.

~~**Differentially private shaping.**~~ **Differentially private shaping.** Unlike constant shaping~~and variable-but-static shaping, dynamic shaping offers the most flexibility for adapting traffic shapeat runtime based on workload patterns and, therefore, can significantly reduce~~, variable shaping can adapt traffic shape, potentially based on runtime workload patterns, and thus significantly reduce shaping overheads. Unfortunately, existing ~~dynamic~~ variable shaping techniques either have unbounded privacy leaks~~or~~, offer only weak privacy guarantees, or require extensive profiling of an application's network traces. NetShaper's novel differential privacy (DP) based shaping strategy provides quantifiable and tunable bounds on privacy leaks, without relying on profiling of application traffic (G2). ~~The DP guarantees are enforced on streams at the granularity of a sliding window of configurable length . Streams longer than this window length retain (weaker) DP guarantees through composition~~NetShaper shapes an application's traffic in periodic, fixed-length *shaping intervals* and provides DP in the length of the application byte stream (burst) accumulated within each interval. The DP guarantees compose over sequence of multiple intervals, thus providing DP for streams of arbitrary duration.

~~**Shaping in a middlebox.**~~ **Shaping in a middlebox.** NetShaper uses a tunnel abstraction to implement traffic shaping. The tunnel shapes application traffic such that an adversary observing the tunnel traffic cannot infer application secrets. In principle, a tunnel endpoint could be integrated with the application host (e.g., in a VM isolated from the end-host application) or in a separate node through which the application's traffic passes. NetShaper relies on the second approach and implements the tunnel endpoint as a middlebox, which could be integrated with an existing network element, such as a router, a VPN gateway, or a firewall. The middlebox implementation enables securing multiple applications without requiring modifications on individual end hosts (G4). Furthermore, it allows pooling multiple flows with the same privacy requirements in the same tunnel, which helps to amortize the per-flow overhead (G3).

~~**Minimal modifications to end applications.**~~ **Minimal modifications to end applications.** By default, NetShaper shapes all traffic through a tunnel with a fixed differential privacy guarantee. However, an application can explicitly specify different DP parameters to adapt the privacy guarantee enforced for its traffic, as well as bandwidth and latency constraints and any prioritization preferences on a per-flow basis. This requires only a small modification in the application; it must transmit a shaping configuration message to the middlebox. Thus, NetShaper offers a balance between being fully application-agnostic and optimizing for privacy or overhead with minimal support from applications (G2, G5).

2.3 Threat Model

NetShaper's goal is to hide the content of an application's network traffic. Hiding the type of traffic [63], the communication protocol [30,80], or the application identity [23,29,35] are non-goals, although NetShaper can adapt its shaping strategy to address these goals. The applications are non-malicious and do not leak their own secrets.

We assume that the application endpoints are inside separate trusted private networks (e.g., each node is behind a

VPN gateway node) . We assume that the applications are non-malicious and do not leak the secrets themselves.

and the adversary cannot infiltrate the private network, or the clients and servers within it. (Thus, we exclude covert attacks [8] and colocation-based attacks [49,61]). The adversary controls network links in the public Internet (e.g., ISPs) and can record, measure, and tamper with the victim application's traffic as it traverses the links under the adversary's control. The adversary can precisely record the traffic shape—the sizes, timing, and direction of packets—between the gateway nodes. In particular, it may have access to observations of arbitrary known streams to train its attack. Furthermore, the adversary can drop, replay, or inject packets into the victim's traffic. However, it cannot infiltrate the private network, or the clients and servers within the private network (thus, no covert attacks). It may also have knowledge about NetShaper, including its shaping strategy and privacy configurations.

We do not consider threats due to observing the IP addresses of packets [36], although NetShaper can hide IP addresses of application end hosts applications behind a shared traffic shaping tunnel. We also do not consider the threat where a victim accidentally installs a malicious script in the browser, thus enabling an adversary to colocate with the victim's application and observe its traffic . This is a reasonable assumption, since a colocated adversary can exploit many other direct or indirect channels for data leaks that will be far more efficient than network side channels .

NetShaper does not address leaks of one application's sensitive data through the traffic shape of colocated benign applicationstransmitting only non-sensitive traffic. Such leaks can arise, for instance, due to microarchitectural interference among the applications colocated on a host or among their flows if they pass through shared links. NetShaperassumes that privacy-sensitive and privacy-insensitive applications are physically isolated and their flows use separate network paths. In practice, the end hosts could instead implement side-channel End hosts could implement orthogonal mitigations against colocated applications [16,43,49,56,64,71] and combine NetShaper's traffic shaping with TDMA scheduling on network links [13,72].

We present a middlebox-based NetShaper implementation that can be placed in front of integrated with an organization's trusted gateway router. NetShaper's trusted computing base (TCB) includes all components in the organization's private network and the middleboxes. We do not address leaks of secrets due to bugsBugs, vulnerabilities or side channels in the middleboxes . In practice, these that threaten traffic confidentiality could be mitigated using orthogonal techniques, such as software fault isolation [69], resource partitioning [46], and constant-time implementation techniques [7,22,81].

Under these assumptions, NetShaper prevents leaks of application secrets through the sizes and timing of packets transmitted in either direction between the application endpoints.

0

2.4 A Primer on Differential privacyPrivacy

We use Differential Privacy (DP) to quantify the privacy of our shaping mechanism. DP is a technique originally developed in the context of databases. DP adds noise to computations performed on this database (e.g., counts, averages), such that an adversary cannot learn specific information about records in the database from the DP computation's result.

Formally, a randomized algorithm $\mathcal{M}$ is (ε,δ)-DP with respect to a distance metric ρ over databases if for all $\mathcal{S} \subseteq \text{Range}(\mathcal{M})$ and for all databases d, d' such that differ in only one element $\rho(d,d') \leq 1$, we have:

$$P(\mathcal{M}(d) \in \mathcal{S}) \leq \exp(\varepsilon) P(\mathcal{M}(d') \in \mathcal{S}) + \delta.$$

Intuitively, changing one element from the database that mechanism $\mathcal{M}$ runs on does not drastically change the probability of a given output. Enforcing this constraint provably prevents membership inference (learning that a specific user contributed data to the database) and reconstruction attacks (reconstructing a row of the database) . The strength of the privacy protection is parameterized by two parameters. ε represents the privacy loss of algorithm $\mathcal{M}$, while δ can be understood as a failure probability (set to an appropriately small number). For both parameters, smaller means more private.

Although this standard definition of DPprivacy for databases employs the Hamming metric, which counts the number of different entries, the theory can be extended to other distance metrics . We leverage this in NetShaperto parameterize the granularity at which we offer privacy guarantees over streams (§3).

Our shaping mechanism relies on three fundamental properties of DP . First, DP is resilient to post-processing: given the result of any (ε,δ)-DP mechanism$r \sim \mathcal{M}$, any function $f(r)$ of the result is also (ε,δ)-DP. As a result, any computation or decision made on a DP result is still DP with the same strength. Second, DP is closed under adaptive sequential composition. The combined result of DP mechanisms $\mathcal{M}_1$ and $\mathcal{M}_2$ is also DP, though with weaker (higher) ε Finally, we provide a brief primer on DP, the steps involved in building a DP mechanism, and δ. We compute DP composition results using Rényi-DP to achieve strong composition results, that can subsequently be converted back to the standard definition of differential privacy. Third, DP is robust to auxiliary information: the guarantee from eq. 1 holds regardless of any side information known to an attacker.

3 Differentially Private Traffic Shaping

The adversary can observe sizes, inter-packet intervals, and directions of packets in sequences of arbitrary lengths.

~~Given these observations, the specific DP guarantee that NetShaper~~the key properties of DP that are relevant in the context of traffic shaping (§3). ~~provides is that the adversary cannot identify (i) the traffic content (e.g., video streams, web pages), and (ii) the presence of any one flow between two application endpoints. We start with a brief primer on DP and its key properties (§2.4).We then formalize the information available to an adversary observing an application's traffic and describe our building blocks for a differentially private shaping mechanism in §??. We describe our mechanism for sending data based on DP in §3.2 and prove our guarantees in §??.~~

2.1 ~~A Primer on Differential Privacy~~

Developed originally for databases, DP is a technique to provide aggregate results ~~on a database~~ without revealing information about individual database records. Formally, a randomized algorithm $\mathcal{M}$ is (ε,δ)-DP if, for all ~~$\mathcal{S} \subseteq \text{Range}(\mathcal{M})$~~ $\mathcal{R} \subseteq \text{Range}(\mathcal{M})$ and for all *neighboring* databases d, d' that differ in only one element~~, we have:~~:

$$P[\mathcal{M}(d) \in \mathcal{R}] \leq e^{\varepsilon} P[\mathcal{M}(d') \in \mathcal{R}] + \delta \qquad (1)$$

The parameter ε represents the *privacy loss* of algorithm $\mathcal{M}$, i.e., given a result of $\mathcal{M}$, the information gain for any adversary on learning whether the input database is d or d' is at most e^{ε} [41]. The δ is the probability with which $\mathcal{M}$ fails to bound the privacy loss to e^{ε}.

Building such a randomized DP algorithm $\mathcal{M}$ involves three main steps: (i) defining neighboring database states, (ii) defining a database query and determining the sensitivity of the query to changes in neighboring databases, and (iii) adding noise to the query. Neighboring databases d and d', as mentioned above, are characterized by the *distance* between the databases, which quantifies the granularity at which the DP guarantee applies. Traditionally, this distance is defined as the number of records that differ between d and d'. However, DP also extends to other neighboring definitions and distance metrics used in specific settings [19, 45].

Given a database query q, the sensitivity of the query Δq is the max difference in the result achieved when the query is executed on the neighboring databases d and d'. Intuitively, a larger Δq implies higher probability of an adversary inferring from a result the database on which the query was executed, thus incurring higher privacy loss. To mitigate this privacy loss, a DP mechanism therefore adds noise to the query result to hide the true result and the underlying database. Popular noise mechanisms are Laplace [28, §3.3] and Gaussian [25].

DP provides three properties. As we will show in §3.2, these are also of relevance to NetShaper's DP traffic shaping. First, DP is resilient to post-processing: given the result r of any (ε,δ)-DP mechanism $\mathcal{M}$, any function $f(r)$ of the result is also (ε,δ)-DP. As a result, any computation or decision made on a DP result is still DP with the same guarantees. Second, DP is closed under adaptive sequential *composition*: the combined result of two DP mechanisms $\mathcal{M}_1$ and $\mathcal{M}_2$ is also DP, though with higher losses (ε and δ). We use the Rényi-DP definition [51] to achieve simple but strong composition results and subsequently convert the results back to the standard DP definition. Third, DP is robust to auxiliary information: the guarantee from Equation 1 holds regardless of any side information known to an attacker. Therefore, attacker's knowledge of shaping mechanism does not affect its privacy guarantees That is, an attacker knowing or controlling part of the database cannot extract more knowledge from a DP result than without this side information.

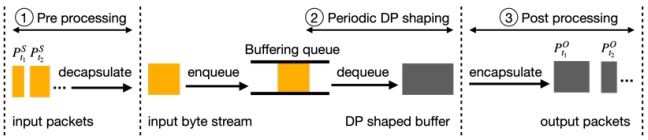

Figure 1: Overview of DP shaping

3 Differentially Private Traffic Shaping

3.1 ~~The Building Blocks~~

The goal of differentially private shaping is to dynamically adjust packet sizes and timing based on the available data stream, while ensuring that the DP guarantees hold for any information that an adversary (§2.3) can observe.

~~Figure 1 illustrates NetShaper's (ε,δ)-DP shaping strategy. An~~ We first formally model an application's input stream ~~is~~ as a packet sequence ~~$S = \{P_1^S, P_2^S, P_3^S, \ldots\}$, where $P_i^S = (l_i^S, t_i^S)$~~ $S = \{P_1^S, P_2^S, P_3^S, \ldots\}$, where $P_i^S = (l_i^S, t_i^S)$ indicates that the i^{th} input packet in ~~S has length l_i~~ S has length l_i^S bytes and is transmitted at timestamp ~~t_i~~ t_i^S. We call the total duration of a finite stream $\tau^S \triangleq \max t_i^S - t_1^S$. Without shaping, an adversary can precisely observe S and infer the content, which is correlated with the stream ~~(~~§2.1).

~~Our DP shaping relies on two key ideas. First, it models the DP guarantees for the (potentially long) traffic streams in windows~~ Figure 1 provides a high-level overview of the differentially-private shaping mechanism. Shaping happens in periodic intervals of fixed length ~~W, denoted by $(\varepsilon_W, \delta_W)$-DP. An input sequence over window j is a finite subsequence $S_j \subset S$, such that $S_j = \{P_i^S \mid P_i^S \subset S \text{ and } t_i \subset j\}$.~~ T, called the ~~NetShaper~~*DP shaping intervals*. ① As the packets in an application's stream arrive, the payload bytes extracted from the packets are placed into a *buffering queue*. ② In each periodic interval, the DP shaping algorithm performs a *DP query*~~'s DPguarantees all (overlapping) windows up to size W.~~

~~A key assumption for~~ : it measures the length of Q with DP, to determine the number of bytes to transmit in the next

interval. NetShaper ~~'s DP guarantees to hold over W-sized windows In other words, we assume: All bytes enqueued at time t are transmitted by time $t+W$. We explain how to realize this assumption in a tunnel design in §4. Under this assumption, the privacy loss of the complete traffic stream is simply a DP compositionof the privacy losses over consecutive windows.~~ then prepares a DP shaped buffer using the payload bytes from Q, and additional dummy bytes if required. This shaped buffer is enqueued to be sent over the network at the end of the DP shaping interval, right before the next interval starts. ③ Finally, data in the shaped buffer may be split into one or more packets, as part of a post-processing step, and transmitted to the network.

~~The window length W is a configuration parameter, which is set before the start of an application's transmission. In practice, W would be in the order of~~ The size of each shaped buffer generated in an interval has $(\varepsilon_T, \delta_T)$-DP guarantees. With DP composition, the per-interval guarantees compose over a ~~few seconds~~sequence of multiple intervals, thus providing DP guarantees for traffic streams of arbitrary lengths.

We now discuss the steps of building a DP mechanism for traffic streams in §3.1 and the privacy guarantees in §3.2.

~~Secondly, we use the primitive of a~~

3.1 DP for Traffic Streams

We now discuss the three steps for building a DP mechanism on traffic streams. Specifically, we present our neighboring definition for streams, define the DP query on streams that ~~buffering queueto control the maximum information accessible by an adversary within each window. We denote the number of bytes present in the queue (i.e., length of the queue) by L. Conceptually,~~ NetShaper ~~extracts bytes from the input stream, S, and enqueues them. The shaped traffic is then transmitted as a packet sequence denoted by $O = \{P_1^O, P_2^O, P_3^O \ldots\}$, which is observable by an adversary.~~ runs and bound its sensitivity, and show the DP mechanism that we use to make the query DP.

~~In the rest of this section, we focus on~~ **Step 1: Neighboring Definition.** Building a DP mechanism requires a suitable definition of neighboring streams, which requires a notion of distance between streams. The neighboring definition has two implications. First, it determines the sensitivity for a "query" subject to the DP mechanism and, in turn, the amount of noise necessary for ensuring a given DP guarantee. Second, it defines the granularity of privacy guarantee: intuitively, neighboring streams are indistinguishable based on only the results of the DP mechanism applied to them. Hence, we aim for a neighboring definition for which "streams have many neighbors", and the sensitivity of the DP query we want to run is as low as possible.

Defining neighbors over streams has two challenges. First, the streams can be arbitrarily long and the distance between streams would typically increase with stream length. Secondly, if we consider streams with packet timestamps at the finest granularity, the distance between the streams may be as large as the sum of sizes of all packets in both streams. Both these factors imply that a stream would either have few neighbors (enabling weak privacy), or the neighboring definition would need to specify a large distance threshold, requiring a lot of noise for strong DP guarantees.

To keep the neighboring distance threshold small, we take two steps. First, we define the notion of a ~~NetShaper's DP guarantees over a single window. We first formally define a notion of $(\varepsilon_W, \delta_W)$-DP privacy, which guarantees DP over transmission windows of~~ *neighboring window*, which is a time interval of configurable length W ~~. The guarantee applies over all~~ over input streams. For notational convenience, we set W ~~windows, and applying DP composition yields guarantees over multiple windows. Then, we provide an overview~~ as an integral multiple of the DP shaping ~~mechanism, which further samples noise in multiple shorter uniform intervals within each window. Finally, we prove how the shaping mechanism provides $(\varepsilon_W, \delta_W)$-DP.~~ interval T and write $W = kT$, although this is not a strict requirement.

~~To formalize NetShaper's DP guarantees, we first define a meaningful distance between any pair of streams in windows of length W and the associated~~ Secondly, to measure the distance between streams over a neighboring window, we consider the total bytes in each stream (burst lengths) transmitted within coarse-grained time intervals and use the difference in the burst lengths in the intervals within the window. Intuitively, we need an interval granularity that is coarse enough to generate similar burst length sequences in more streams, but is also small enough to bound the accumulation of differences over time (to bound sensitivity, our next step). As will become clear with Proposition 1, the DP shaping interval T is the coarsest granularity that we can use. Hence, considering a neighboring window starting at a timestamp t_w, i.e., $[t_w,\ t_w + W)$, we define the following representation of stream S over the window $[t_w,\ t_w + W)$ at granularity T: $S_{t_w,W} = \{L^S_{t_w}, L^S_{t_w+T}, L^S_{t_w+2T}, \ldots, L^S_{t_w+(k-1)T}\}$, where $L^S_t \triangleq \sum_{(l_i^S, t_i^S)\in S} \mathbb{1}\{t_i^S \in [t, t+T)\} l_i^S$ is the total application bytes accumulated in Q in the interval $[t, t+T)$.

We now present the following neighboring definition:

Definition 1. ~~*Two streams S_j and S'_j transmitted in a window j*~~ *Two streams S and S' are neighbors if~~their ~~, for any neighboring window $[t_w,\ t_w + W)$, the* L1-norm ~~*distance is at most Δ_W bytes in , i.e., $\| S_j - S'_j \|_1 \leq \Delta_W$.*~~

~~*Δ_W is the max L1-norm*~~ *distance between ~~each pair of application streams transmitted in any window j.~~ their representations $S_{t_w,W}$ and $S'_{t_w,W}$ is less than Δ_W. Formally, S and S' are neighbors if:*

$$\max_{t_w} \| S_{t_w,W} - S'_{t_w,W} \|_1 \leq \Delta_W. \tag{2}$$

We utilize the L1-norm (the sum of absolute values) ~~as~~

~~our distance metric~~ to quantify the ~~dissimilarity~~ distance between two traffic streams, as it captures differences in both ~~packet sizes and~~ traffic size and temporal alignment, at the granularity of T. We will show (in Prop 1) that despite our restriction of defining neighboring streams at a granularity of T, and of computing distances over windows of length W, we can quantify NetShaper's DP guarantees for streams at any granularity and of any length.

3.2 ~~The Shaping Mechanism~~

The neighboring window length W and neighboring distance Δ_W are both configuration parameters, which are set before the start of an application's transmission. In practice, W would be in the order of milliseconds to seconds. Subsequently, one would determine Δ_W based on the typical difference of traffic between application streams over windows of length W. The practical upper bound for Δ_W is the NIC's line rate times window length W, but smaller values based on domain knowledge are often possible.

~~To apply noise in each interval, we now define the sensitivity~~ **Step 2: DP query and sensitivity.** In NetShaper, a DP query measures the buffering queue length L with DP at intervals T. This noisy measurement determines the number of bytes that must be transmitted in the interval. To make the measurement of L differentially private, we need to bound the sensitivity Δ_T of the queue length ~~over intervals of length T. Sensitivity, denoted~~ variable L. This sensitivity Δ_T ~~,~~ is the maximum difference in ~~the queue length over any interval T~~ L that can be caused by changing one application stream to ~~another~~neighboring one. Formally, consider two alternative ~~streams S_j and S'_j~~ neighboring streams S and S' passing through the queue. Suppose that when transmitting ~~S_j (similarly S'_j~~S (similarly S'), the queue length at ~~the beginning of its~~ time k ~~th interval~~ is denoted by L_k (respectively L'_k). Then, assuming w.l.o.g. that $k \geq k'$:

$$\Delta_T = \max_{k=0}^{\lceil \frac{W}{T} \rceil \tau} \max_{S_j, S'_j, S, S'} |L_k - L'_k| \qquad (3)$$

~~**Shaping overview.** NetShaper's DP shaping involves three steps as shown in Figure 1. As application packets arrive in a window w,~~ Bounding Δ_T is still challenging though, as our neighboring definition only bounds the difference in traffic between two streams over any window of length upto W. Because of this, when $\tau >> W$, differences between what S and S' would enqueue in Q can accumulate over time, and the difference betwen L_t and L'_t can grow unbounded over time.

To bound Δ_T, NetShaper relies on the key assumption that the tunnel can always transmit all incoming data from application streams within any W-sized time window. That is,

Assumption 1. *All bytes enqueued prior to or at time t are transmitted by time $t + W$.*

To enforce this assumption, NetShaper implements a time to live in the ~~preprocessing step extracts the payload bytes and enqueues them into the~~ buffering queue, flushing all bytes older than W from Q (see §4 for more details). Intuitively, this assumption caps the accumulation of traffic differences in Q to the maximum difference over W, i.e., Δ_W. Since the size of Q cannot differ by more than Δ_W when changing a stream by a neighboring one, the difference between DP query results of Q under two neighboring streams—which is the sensitivity of the DP query, Δ_T—is upper-bounded by Δ_W. Formally:

Proposition 1. *NetShaper enforces $\Delta_T \leq \Delta_W$. ~~In a periodic interval k, the core DP shaping algorithm samples noise~~*

Proof sketch. Consider any two streams S_j and S'_j, as in Equation 3. The proof proceeds in two steps. First, under Assumption 1, streams can accumulate queued traffic for at most W, so two different streams can create a difference $|L_k - L'_k|$ of at most Δ_W. Second, dequeuing can only make two different queues closer: Consider query time k, with queue lengths $L_k > L'_k$ (the opposite case is symmetric). For a DP noise draw z~~from a DP distribution and computing a DP burst size $\tilde{L}_k \triangleq L_k + z$. The shaping logic then prepares~~, we have $\tilde{L}_k > \tilde{L}'_k$. Since shaping sends at least as much data under $\tilde{L}_k$ as under $\tilde{L}'_k$, but no more than $\tilde{L}_k - \tilde{L}'_k$, after dequeuing we have $|L'_{k+1} - L_{k+1}| \leq |L'_k - L_k|$. In summary, the maximum queue difference under two different streams Δ_T can grow to at most Δ_W due to data queuing, and dequeuing only decreases that difference, and hence $\Delta_T \leq \Delta_W$. The complete proof is in §B. □

Step 3: Adding Noise. With sensitivity bounded at Δ_W, we can now query L with DP using an additive noise mechanism, which entails sampling noise z from a DP distribution and computing the DP buffer queue length as $\tilde{L}_k \triangleq L_k + z$. Specifically, NetShaper uses the Gaussian mechanism, in which the noise z is sampled from a ~~normal distribution $\mathcal{N}(\mu, \sigma^2)$~~ centered normal distribution $z \sim \mathcal{N}(\mu, \sigma^2)$, where the variance is parameterized by ε_T, δ_T, and ~~Δ_T: The mean μ is 0 and the variance σ^2 is given by $\frac{2\Delta_T^2}{\varepsilon_T^2} \ln(\frac{1.25}{\delta_T})$. Given this noise distribution, one measurement is $(\varepsilon_T, \delta_T)$-DP. Data in the~~ Δ_W: $\sigma^2 = (2\Delta_W^2)/(\varepsilon_T^2)\ln(1.25/\delta_T)$. Parameters ε_T, δ_T determine the amount of noise added to each DP query result.

3.2 Privacy Analysis

The previous section defines $(\varepsilon_T, \delta_T)$-DP guarantees for the traffic transmitted in an individual shaping interval. We now discuss (i) the guarantees for longer application streams, (ii) the guarantees on a packet-level sequence derived from a shaped buffer sequence, and (iii) the privacy implications for streams that fall outside of the neighboring definition.

Guarantees for streams. Recall from the previous section that shaping happens at intervals T; in each interval we perform a DP query on the buffering queue length L and create

a shaped buffer of length $\tilde{L}$, which is subsequently queued for transmitting over the network at the end of the interval. Enqueueing data into the shaped buffer at the end of each shaping interval creates a sequence of states for the shaped buffer $\{(\tilde{L}_1, T), (\tilde{L}_2, 2T), (\tilde{L}_3, 3T), \dots\}$. Although this sequence is not technically observable by an adversary, this is where we prove our DP guarantees using DP composition over queries performed during the stream transmission.

Proposition 2. *For any stream S of duration $\tau^S \leq \tau$, NetShaper enforces (ε, δ)-DP for the sequence $\{(\tilde{L}_1, T), (\tilde{L}_2, 2T), (\tilde{L}_3, 3T), \dots\}$, with $\varepsilon, \delta \triangleq DP\_compose(\varepsilon_T, \delta_T, \lceil \frac{\tau}{T} \rceil)$.*

Proof. Consider two neighboring streams S and S'. By design, the times at which shaped buffers are queued are independent of application data, so $\{(\tilde{L}'_1, T'), (\tilde{L}'_2, 2T'), (\tilde{L}'_3, 3T'), \dots\} = \{(\tilde{L}_1, T), (\tilde{L}_2, 2T), (\tilde{L}_3, 3T), \dots\}$, and we can restrict our considerations to the sequences $\{\tilde{L}_1, \tilde{L}_2, \tilde{L}_3, \dots\}$ and $\{\tilde{L}'_1, \tilde{L}'_2, \tilde{L}'_3, \dots\}$. By Prop. 1, the sensitivity of each measurement is at most Δ_W. By the Gaussian DP mechanism, the measured queue size $\tilde{L}$ in each interval is $(\varepsilon_T, \delta_T)$-DP. Using DP composition over the $\lceil \frac{\tau}{T} \rceil$ DP queries made during any duration τ yields the (ε, δ)-DP guarantee. □

We use Rényi-DP composition on the Gaussian mechanism for DP_compose(). NetShaper provides a DP guarantee for streams of any length t, with the guarantee degrading gracefully as DP composition (of order $\sqrt{\tau}$ as the length grows).

Guarantees for packet sequences. Data from the shaped buffer is ~~then split into one or more packets and transmitted to the network. Since these~~ sent over the network, transmitted as a packet sequence denoted by $O = \{P_1^O, P_2^O, P_3^O \dots\}$, These packets are a post-processing of the DP-shaped buffer. As long as the packets are generated independently of any secret data, they preserve the DP guarantees of shaping due to the post-processing property of DP. This yields the following result, directly implied by Proposition 2 and DP ~~as long as no new dependency on private data is introduced. This last constraint requires the packets' size and transmit time to be selected independently of the data. We describe how~~ post-processing:

Corollary 1. *For any stream S of duration $\tau^S \leq \tau$, ~~NetShaper~~NetShaper enforces ~~this constraint in §4.2.~~ (ε, δ)-DP for its output packet sequence O, with $\varepsilon, \delta \triangleq DP\_compose(\varepsilon_T, \delta_T, \lceil \frac{\tau}{T} \rceil)$.*

~~The privacy loss (ε_W) and bandwidth overheads of the DP shaping (represented by σ_T, i.e., the standard deviation of the noise distribution function) depend on W~~**Privacy for non-neighboring streams.** Finally, if the distance between two streams is larger than Δ_W, e.g., say $k\Delta_W$ for some factor k, NetShaper still provides a (degraded) DP guarantee through group privacy [28, Theorem 2.2] applied to the Gaussian mechanism. Namely, a DP query in each shaping interval T for the non-neighboring stream provides $(k\varepsilon_T, \delta_T)$-DP, and the guarantees can be extended for the stream duration τ by applying DP composition to this new value.

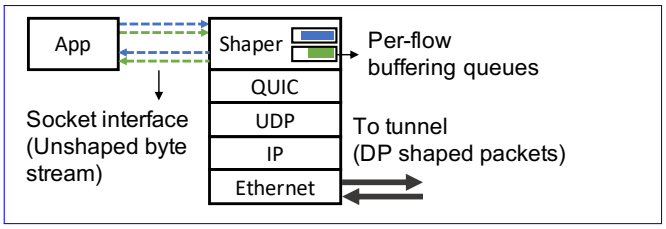

Figure 2: Overview of tunnel design (one endpoint)

Interpretation of the guarantees. NetShaper's shaping algorithm provides a $(\varepsilon_T, \delta_T)$-DP guarantee on the volume of application traffic enqueued (in the buffering queue) in a fixed-length interval (and, by post-processing, the volume of traffic observable on the network). Under perfect timing for the DP shaping interval T, the DP guarantee ensures that two neighboring streams, i.e., their contents, are indistinguishable with the probability as defined in Equation 1. Smaller ε_T and δ_T implies higher noise in shaping, which increases the uncertainty about the original stream in the shaped traffic.

Secondly, to enforce the DP guarantees, the DP noise of the Gaussian mechanism does not depend on the total number of flows. Intuitively, the DP guarantee is shared among all the streams multiplexed through the buffering queue simultaneously for a fixed amount of noise, and the overhead (i.e., noise added) gets amortized among the streams.

Privacy vs Performance. NetShaper's shaping mechanism introduces several parameters which impact privacy and performance, specifically latency and bandwidth overheads. These parameters include ε_T, δ_T, Δ_W, W, and ~~the number of intervals $N = \lceil \frac{W}{T} \rceil$ in W.~~ T. Larger Δ_W requires lower ε_T for stronger privacy, which implies noisier measurements. Noisy measurements imply more overhead—when the noise is positive, dummy bytes need to be sent, incurring higher bandwidth overhead; when the noise is negative, fewer bytes are sent and the unsent bytes accumulated in the buffering queue incur a latency overhead. This is the privacy-overhead trade-off we expect from DP.

Additionally, the ~~latency overheads depend on~~ parameters T ~~. Note that for a specific value of Δ_W~~ and ~~N,~~ W have a more subtle impact on the ~~DP guarantee ε_W is fully specified by σ_T, and remains the same even at different time scales. That is, scaling~~ privacy-overhead trade-off. Traffic is shaped in intervals of T; thus, T impacts the latency and burstiness of the traffic. A smaller T provides lower transmission latency and smaller bursts per interval. However, it also requires more DP queries and, thus, incurs higher privacy loss when transmitting the complete stream of a given length τ. In practice, one would set T to the maximum value that can minimize privacy

loss while providing tolerable latency.

A large W for a fixed Δ_W implies that neighboring streams can differ by at most Δ_W over a longer window size W and , which weakens the neighboring definition and, hence, the privacy guarantees. While smaller W is desirable, the lower bound is T proportionally does not change the privacy and overhead costs. . Recall that, to bound Δ_T (Assumption 1), NetShaper must drop any bytes left in the buffering queue for longer than W. Since data leaves the buffering queue in each shaping interval after a DP query, setting $W = T$ would lead to immediate dropping of the bytes from the buffering queue that aren't transmitted in response to the DP query. This would happen in each interval where the DP query samples a negative noise value. These data drops would degrade NetShaper's performance in terms of both throughput and latency. Hence, we need $W >> T$ to ensure that data has time to leave the buffering queue before it is too old. Typically, one would set W based on application domain knowledge, such as the maximum size of a web request or the fact that videos often consist of a sequence of segments requested at 5s intervals.

We analyze the impact of different choices for these parameters on the privacy guarantees and overheads in §5. Here, we focus on a formal model of the DP guarantees.

4 Traffic Shaping Tunnel

The previous section describes an abstract differentially private traffic shaping strategy. We now present NetShaper's traffic-shaping tunnel.

A tunnel must address three requirements. First, it must satisfy DP guarantees. For this, the tunnel must complete DP measurements queries and prepare shaped packets within each interval, and it must be able to transmit all payload bytes generated from an application within a finite window length (as defined in the DP strategy). Secondly, the payload and dummy bytes in the shaped packets must be indistinguishable to an adversary. For this, the payload and dummy bytes must be transmitted through a shared transport layer so that they are identically acknowledged by the receiver and subject to congestion control and loss recovery mechanisms. Finally, the tunnel must provide similar levels of reliability, congestion control, and loss recovery as expected by the application.

Overview of tunnel design (one endpoint)

Figure 2 shows the design of one endpoint of NetShaper's traffic shaping tunnel. A similar endpoint is deployed on the other end of the tunnel. The shape of the traffic in the tunnel can be configured independently in each direction. The privacy loss in bidirectional streams is the DP composition of the privacy loss in each direction.

A tunnel endpoint consists of a shaping layer (Shaper) on top of QUIC, which in turn runs on top of a standard UDP stack[1]. The tunnel endpoints establish a bidirectional QUIC connection and generate DP-sized transmit buffers in fixed intervals, which carry payload bytes from one or more application flows. In the absence of application payload, a tunnel endpoint transmits dummy bytes, which are discarded at the other endpoint. QUIC encrypts all outbound packets.

NetShaper adopts a transport-layer proxy architecture: each application terminates a connection with its local tunnel endpoint. The application byte stream is sent to the remote application over three piecewise connections: (i) between the application and its local tunnel endpoint, (ii) between the tunnel endpoints, and (iii) between the remote tunnel endpoint and the remote application. This ensures only one active congestion control and reliable delivery mechanism in the tunnel and that all bytes are subject to identical mechanisms[1].

The application and the tunnel endpoint shown in Figure 2 could either be colocated on the same host or located on separate hosts. For example, the tunnel endpoint could be on a separate middlebox or integrated with a gateway at the edge of an organization's network. In each case, the traffic between the application and the tunnel endpoint is assumed to be unobservable to an adversary. Our design (§4.1) does not distinguish between the two configurations. Our implementation (§4.2) assumes that the tunnel endpoint is located on a separate middlebox. We discuss security in §4.3 and alternate deployments in §4.4.

4.1 Tunnel Design and Operations

Tunnel setup and teardown. **Tunnel setup and teardown.** Before applications can communicate with each other, a NetShaper tunnel must be set up between their local tunnel endpoints. The initiator application sends a configuration message to its local tunnel endpoint with the source and destination IP addresses and ports, a reliability flag, and a privacy descriptor. The reliability flag indicates if the tunnel should provide reliable delivery semantics or not. The privacy descriptor indicates the DP parameters to be used for shaping the tunnel traffic.

Upon receiving a configuration message, the Shaper establishes a QUIC connection with the remote tunnel endpoint and configures the reliability semantics and privacy parameters for each direction. It also initializes three types of bidirectional streams in the tunnel: control, dummy, and data streams. One *control stream* is used to transmit messages related to the establishment and termination of a connection between the application endpoints. A *dummy stream* transmits padding in QUIC packets in the form of STREAM frames[2]. The tunnel pre-configures a finite number of data streams, which carry payload bytes from one or more application flows.

[1] Instead of QUIC/UDP, NetShapercould also use a traditional TCP stack.

[1] We discard tunneling TCP through TCP as it causes TCP meltdown [4, 37], or TCP through UDP as it is unsafe. (TCP between the application hosts would retransmit lost payload bytes only, not any dummy bytes injected between the tunnel endpoints, making the dummy bytes observable.)

[2] We do not use QUIC's PADDING frames as they do not elicit acknowledgements and hence are distinguishable from STREAM frames [39].

When the tunnel is inactive for a period of time, one of the tunnel endpoints initiates a termination sequence and closes all open QUIC streams and the tunnel connection.

~~**Connection establishment and termination.**~~ **Connection establishment and termination.** Once a tunnel is ready, applications can establish and terminate connections with each other, which is mediated by the tunnel. When the initiator application runs a connection establishment handshake with its local tunnel endpoint, the Shaper maps the application flow to a per-flow buffering queue and one of the inactive QUIC data streams in the tunnel, and notifies the remote tunnel endpoint. The remote tunnel endpoint establishes a connection with the receiver application and maps the receiver application's flow with the data stream. The connection termination handshake is handled similarly by the tunnel endpoints. The messages for connection establishment and termination are transmitted over the control stream in the tunnel and shaped according to the tunnel's parameters.

~~**Outbound traffic shaping.**~~ **Outbound traffic shaping.** The Shaper accumulates the outbound bytes of an application flow in a buffering queue before it transmits them in packets whose sizes and timing follow a distribution that guarantees DP. Within a tunnel, the Shaper transmits bytes from all active flows into a differentially-private packet sequence. At periodic intervals, called DP shaping intervals, it performs a DP ~~measurement~~ query on the per-flow queues to determine the number of bytes $\tilde{L}$ to be transmitted according to the tunnel's DP parameters. It prepares a *shaped buffer* consisting of R payload bytes and D dummy bytes, where R is the minimum of $\tilde{L}$ and the application bytes available in the buffering queues, and $D = \tilde{L} - R$, which may lie between 0 and $\tilde{L}$. The Shaper then passes the buffer with the position and length of the padding to QUIC.

QUIC transforms the shaped buffer into one or more STREAM frames based on the congestion window, the flow window of the receiver endpoint, and the MTU (maximum transmission unit). It places the padding bytes into a dummy STREAM frame. QUIC packages the frames into packets, whose length is at most MTU minus the length of the headers and whose payload is encrypted. QUIC forwards the packets to the UDP layer, which subsequently transmits the prepared packets as quickly as it can, given the line rate of the NIC.

~~NetShaperconfigures the interval such that the Shaper can prepare each shaped buffer within an interval. If the preparation time for a buffer exceeds the interval, the Shaper discards the buffer. This ensures that the buffering queue length does not grow significantly, which in turn controls the overhead incurred due to DP shaping. We evaluate the impact of the length of the buffering queue~~ To enforce Assumption 1, the Shaper tracks the expiry time of each byte enqueued in Q based on the arrival time and the ~~on privacy guarantees, bandwidth overheads, and latency overheads in~~

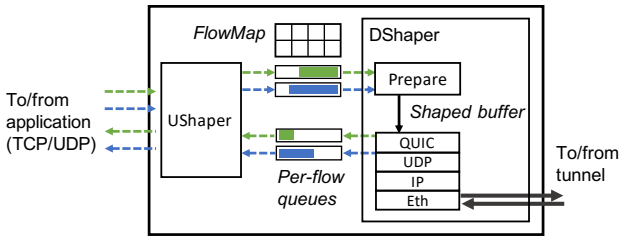

Figure 3: NetShaper middlebox design

§~~5~~neighboring window length W configuration. The Shaper drops the untransmitted bytes in the queue upon their expiry.

~~**Inbound traffic processing.**~~ **Inbound traffic processing.** A tunnel endpoint receives shaped packets from the tunnel and applies inverse processing on each packet. QUIC receives the packet and sends an ACK to the sender. Subsequently, it decrypts the packet, discards the dummy frame, and forwards the payload bytes from the remaining STREAM frames to the application.

4.2 Middlebox Implementation

We present a middlebox-based NetShaper implementation. ~~Recall from §2.2, a middlebox can support shaping for several applications and amortizes the shaping cost among multiple flows that share the same tunnel. Moreover, middleboxes can support "long-term" tunnels between endpoints. Such tunnels may be set up, for instance, between organization campuses to secure all communication between the campuses without the need for modifying individual application hosts.~~

For ease of implementation, our prototype requires applications to explicitly connect to the middleboxes. In principle, NetShaper can transparently proxy application connections.

In our implementation, a middlebox consists of two userspace processes. The `UShaper` mediates *unshaped* traffic between the applications and the middleboxes. The `DShaper` handles *DP shaped* traffic within the tunnel.

~~**UShaper.**~~ **UShaper.** The `UShaper` implements a transport server (or client) for interfacing with each local client (or server, respectively) application[3]. For managing multiple flows, it shares a `FlowMap` table with the `DShaper`, which consists of an entry for each end-to-end flow. Each entry maps the piecewise connections with a pair of transmit and receive queues to carry the local application's byte stream, and shaping configurations (e.g., privacy descriptor) provided by an application at the time of flow registration.

The `UShaper` receives the outbound traffic from a sender application and enqueues the byte stream into a per-flow

[3] ~~The `UShaper` could also be a SOCKS5 proxy.~~

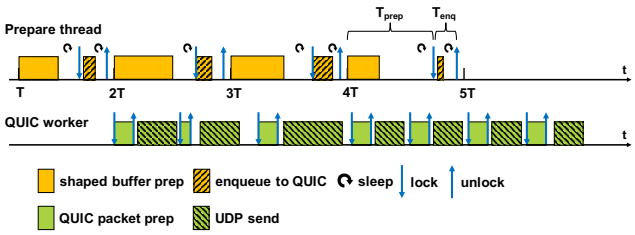

Figure 4: DShaper schedule

transmit queue shared with the DShaper. It also dequeues bytes from a per-flow receive queue, repackages them into transport packets and sends them to the receiver application.

~~**DShaper.**~~ **DShaper.** The DShaper consists of a Prepare thread and a QUIC worker thread. The Prepare thread instantiates a QUIC client/server to establish a tunnel with the remote middlebox and implements the DP shaping logic. On the transmit side, Prepare prepares shaped buffers based on DP queries on the transmit queues and then submits shaped buffers to the QUIC worker for transmission. On the receive size, the QUIC worker transmits ACK frames to the sender and then decrypts the QUIC packets, extracts the STREAM frames, and copies bytes (including dummy bytes) from each frame into the appropriate per-flow receive queue.

~~**Ensuring secret-independent shaping.**~~ **Ensuring secret-independent shaping.** To enforce DP guarantees, DShaper should *transmit* exactly $\tilde{L}$ bytes in each DP shaping interval T. This would require ensuring: **P1.** Prepare computes $\tilde{L}$, allocates and prepares a buffer of length $\tilde{L}$, and passes the buffer to the QUIC worker within T, **P2.** the QUIC worker prepares encrypted packets from the buffer and sends them to UDP, such that the total payload size of the QUIC packets prepared in T is $\tilde{L}$, and **P3.** the UDP stack transmits packets totaling to $\tilde{L}$ payload bytes to the NIC in T. Enforcing all these properties would ~~produce a~~ require a constant-time implementation for each step, which is non-trivial, or a strict time-triggered schedule for each ~~component~~step, which would significantly reduce link utilization and increase packet latencies.

Thanks to DP post processing, however, it suffices to ensure the property P1, and **P4.** that the QUIC worker transforms the shaped buffer into network packets independently of the application data. No other constraint on the sizes and timing of network packets is required to preserve DP.

Satisfying P1 involves one challenge. Although the application is physically isolated from the middlebox, its flow control behavior could be secret-dependent and could affect the middlebox's execution. For instance, the presence or absence of payload traffic from an application can affect the time DShaper requires to prepare the shaped buffers.

Thus, DShaper satisfies P1 as follows ~~. (See~~ (see Figure 4 for reference.) First, Prepare guarantees that $\tilde{L}$ is computed with a DP query in each interval. Secondly, Prepare guarantees that a shaped buffer of length $\tilde{L}$ is *prepared* within a fixed time T_{prep} within each interval~~T~~. Thirdly, Prepare locks the shaped buffer for a fixed time, T_{enq}, during which it enqueues the buffer for a QUIC worker. This ensures that the buffer is completely enqueued before QUIC starts transmitting it and that QUIC receives the buffer only at fixed delays.

We empirically profile the time taken by Prepare for preparing and enqueueing shaped buffers for various DP lengths. We set T_{prep} and T_{enq} to maximum values determined from profiling, and T to the sum of these maximum values, i.e., T_{max}. If Prepare takes time less than T_{prep} (or T_{enq}, respectively) to prepare (or enqueue) a shaped buffer, it sleeps until the end of the interval before moving to the next phase.

To satisfy P4, Prepare and QUIC worker threads run on separate cores sharing only the shaped buffers. UShaper runs on yet a different core and shares the FlowMap and the per-flow transmit queues containing unshaped traffic only with Prepare. It shares the per-flow receive queues with the QUIC worker, but they contain only shaped frames from the QUIC worker. ~~Thus~~Finally, we assume that QUIC encrypts and decrypts shaped buffers in constant-time. With this, the execution of the QUIC worker becomes independent ~~of DP measurements in~~ from Prepare ~~.~~

~~Variations in Prepare's execution due to the state of the per-flow queues are masked by T_{max}, while QUIC's execution depends only on shaped buffers and thus, is~~ and secret-independent overall. Consequently, the ~~packetization of shaped buffers in the~~ QUIC worker and the UDP stack ~~is secret-independent and any variations~~ can packetize the shaped buffers and transmit the packets at link speed, and any variance in packet transmit times ~~induced due to their execution~~ constitute post-processing noise.

Limitations. Our prototype has two limitations in enforcing secret-independent timing. First, our QUIC implementation uses standard OpenSSL, which may not provide constant-time crypto. However, QUIC can be modified to adopt a constant-time crypto library [1, 2] to overcome this limitation. Secondly, it is difficult to find the true maximum values of T_{prep} and T_{enq} on general-purpose desktops. If Prepare's execution exceeds the profiled max values, it violates the theoretical DP guarantees. However, we note that it is difficult to practically exploit these violations for inferring traffic secrets.

4.3 Security Analysis

NetShaper provides the following security property: an adversary cannot infer application secrets from observing tunnel traffic. This property is ensured by a combination of a secure shaping strategy, the tunnel design, and implementation.

S1. Secure shaping strategy. The tunnel transmits traffic in differentially private-sized bursts in fixed intervals. Thus, the overall shape is DP. The proof of DP is in §B.

S2. Secure tunnel design. (i) The privacy guarantees of a tunnel are configured before the start of application transmission and do not change during the tunnel's lifetime. (ii) The tunnel mediates control between the end hosts, e.g., by transmitting custom connection establishment and termination messages. These messages are subject to the same DP shaping as the payload traffic (§4.1). (iii) The payload and dummy bytes in network packets are indistinguishable because all payload and dummy bytes are packaged into QUIC packets and encrypted uniformly. Moreover, QUIC handles acknowledgements, congestion control, and loss recovery for both payload and dummy bytes uniformly (§4.1).

S3. Secure middlebox implementation. (i) The unshaped traffic between an end host and its local middlebox is not visible to an adversary. (ii) `DShaper` follows the tunnel design in transmitting payload and dummy bytes. (iii) The ~~sizes and timing of transmitted packets are secret-independent, because the~~ time required for `Prepare` to prepare and enqueue shaped buffers is masked to secret-independent times. The ~~subsequent packetization of~~packetization of buffers in QUIC is secret-independent (§4.2) and thus retains DP guarantees after post-processing. Any delays in transmitting the buffers can arise only due to congestion or packet losses in the tunnel network, which are secret-independent events.

4.4 Deployment and Maintenance

NetShaper's tunnel endpoint design and implementation are both very modular and portable. The middlebox components are compatible with all application layer protocols (e.g., HTTPS, QUIC-TLS) and network stacks (e.g., TCP, UDP, QUIC stacks). The `UShaper` could also be implemented as a standard SOCKS5 proxy [3].

A tunnel endpoint could be integrated with any node along an application's network path as long as the application traffic is unobservable until egress from the tunnel. By integrating with a trusted VPN gateway of an organization, network administrators could manage "long-term" tunnels between the organization's campuses and support multiple applications without modifying individual end hosts. For instance, separate tunnels may be configured per-application according to the organizational needs, or configurations may be adapted based on coarse-grained changes in the traffic patterns through the day.

Alternatively, by integrating with end user devices, e.g., with VPN clients, users could instantiate a new bidirectional tunnel with a service before each network activity, choose a different configuration for each tunnel instance, and close the tunnel after completion of the activity. A key requirement would be to secure the tunnel endpoint's execution from any internal side channels on the end host, which would be now more prevalent than in the middlebox setup.

5 Evaluation

Our evaluation answers the following questions. (i) How well does NetShaper mitigate state-of-the-art network side-channel attacks? (ii) What are the overheads associated with varying DP relevant configuration parameters? (iii) What are the packet latency overheads and the peak line rate and throughput sustained by our NetShaper middlebox? (iv) What are NetShaper's overall costs on privacy, bandwidth, client latency, and server throughput for different classes of applications? (v) How do NetShaper's privacy guarantees and performance overheads compare to prior techniques?

For our experiments, we use four AMD Ryzen 7 7700X desktops each with eight 4.5 GHz CPUs, 32 GB RAM, 1 TB storage, and one Marvell AQC113CS-B1-C 10Gbps NIC. We simulate client and server applications on two of the desktops and NetShaper's middleboxes on the other two desktops. The middleboxes are connected to each other via an additional Intel X550-T2 10Gbps NIC on each desktop. The client and server desktops are connected to one of the two middleboxes each via the Marvell NICs, overall forming a linear topology.

We implemented the `UShaper` and `DShaper` processes in 1100 and 1800 lines of C++ code, respectively, and deployed them on Ubuntu OS 22.04.02 (kernel version 5.19). NetShaper relies on the MSQUIC implementation of QUIC, libmsquic v2.1.8, which includes OpenSSL for traffic encryption, contributing an additional 180713 LoC to NetShaper's TCB.

For rapid evaluation, we built a simulator, which implements the `Prepare` thread's DP logic. The simulator transforms an application's original packet sequence (from tcpdump) into a sequence of burst sizes within fixed-length intervals, and outputs a sequence of transmit sizes corresponding to DP ~~measurements~~queries. We confirmed that the bandwidth overheads from the simulator closely match the overheads observed on the testbed. Thus, we report privacy and bandwidth overhead results from the simulator and latency and throughput results from the testbed, unless specified otherwise.

~~For all experiments, we use one baseline setup and one of three NetShaperconfigurations. In the baseline setup (), the client is directly connected to the server. In the simulator setup (), we generated sequences of shaped burst sizes using DP shaping. With NetShaper, the traffic between the client and the server passes through two middleboxes, each implementing `UShaper`and `DShaper`. We consider two configurations of the middleboxes: (i) : `DShaper`does not implement shaping (i.e., neither DP noise sampling nor the fixed length loop interval T_{max}), allowing us to measure the system overheads due to the middlebox implementation, and (ii) : `DShaper`implements the full shaping mechanism.~~

We use two applications for case studies, a video streaming service and a medical web service, which we describe below.

~~Video service.~~ ~~The video streaming service is~~ Both applications are hosted on an Nginx 1.23.4 web server and the

datasets are stored on the host file system.

Video service. The video streaming service is used to serve 100 YouTube videos in 720p resolution ~~. The videos are stored on a standard file system on the host OS and have durations ranging from~~ with 5 min to 130.3 min (median 12.6 min) ~~and sizes ranging from~~ durations and 2.7 MB to 1.4 GB (median 73.7 MB) sizes. We implement a custom video streaming client in Python, which uses one TCP connection for a single stream and requests individual 5s segments ~~synchronously~~ from the service synchronously. Unless specified otherwise, we stream the first 5 min of videos in our experiments. The configuration is in line with that used in prior work [61] and reasonable, given the popularity of short videos [67]. ~~The client uses one TCP connection for a single video stream .~~

~~**Web service.**~~ **Web service.** The web service is ~~also hosted on Nginx 1.23.4 and is~~ used to serve a corpus of 100 static HTML pages of a medical website~~. The web pages are stored on a standard file system on the host OS and have sizes ranging~~ , whose sizes range from 54 KB to 147 KB (median: 90 KB). As a client, we use ~~a~~ modified wrk2 [5] that issues concurrent asynchronous HTTPS GET requests at a specified rate.

For all experiments, we use one baseline setup and one of three NetShaper configurations. In the baseline setup (**Base**), the client is directly connected to the server. In the simulator setup (**NS$_S$**), we generated sequences of shaped burst sizes using DP shaping. With NetShaper, the traffic between the client and the server passes through two middleboxes, each implementing `UShaper` and `DShaper`. We consider two configurations of the middleboxes: (i) **NS$_M$**: `DShaper` does not implement shaping (i.e., neither DP noise sampling nor the fixed length loop interval T_{max}), allowing us to measure the system overheads due to the middlebox implementation, and (ii) **NS**: `DShaper` implements the full shaping mechanism. By default, each middlebox is configured with 128 pairs of per-flow transmit and receive queues (unless specified otherwise). We configure the queue sizes for the max data that can be transmitted at line rate for a given DP shaping interval. We configure a max cutoff for the shaped buffer length based on the max burst length of the application and the number of active flows. This implies that the number of flows is public.

In addition, we compare with two other shaping strategies: constant-rate shaping (**CR**), which is the most secure shaping strategy, and Pacer (**Pacer**), a SOTA system that shapes traffic on a per-request basis. For **CR**, we configure the peak load corresponding to the largest object sizes in our applications, which involves transmitting 1.7MB in 5s for videos and 57KB in 50ms for web. For Pacer, we pad all web pages to the largest page size, i.e., 147KB in our dataset. For videos, Pacer pads a segment at i^{th} index in a video stream to the largest segment size at that index across all videos in the dataset.

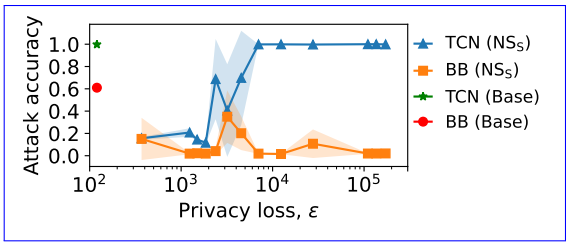

Figure 5: ~~Classifier accuracy on shaped traces.~~ Classifier accuracy on shaped traces.

5.1 NetShaper Defeats Attack Classifiers

We start with an empirical evaluation of the privacy offered by NetShaper's traffic shaping. Recall that the traffic shaping depends on several DP parameters: the window length W, the sensitivity ~~for neighboring streams Δ_W~~Δ_T, the length of the DP ~~measurement~~ interval T, and the privacy loss ~~ε_W.~~ ε. We evaluated the classifiers from §2.1 on shaped traffic generated using various values of these DP relevant parameters. We present the classifiers' performance based on only one set of values for W, Δ_T, and T, while varying ε between [200, 200000]. Our goal is to provide intuition about what values of ~~ε_W~~ ε are sufficient to thwart a side-channel attack.

We set (i) $W = 5s$ to align with the 5s video segments that comprise the videos, (ii) ~~$\Delta_W = 1MB$, which covers 97% of the video streams~~ $\Delta_T = 2.5MB$, which covers 99th %ile of the distances in our dataset (§C), and (iii) $T = 1s$, which leads to composing the privacy loss over $N = 5$ DP ~~measurements of~~ queries on the buffering queues. The ~~interval of~~ 1s interval provides a reasonable trade-off between ~~the privacy lossdue to multiple DP measurements, the bandwidth overhead, and the latency overhead incurred while shaping individual video segments~~privacy loss, and bandwidth and latency overheads, which we discuss in the subsequent sections.

We used 40 videos of 5 min duration each. We streamed each video 100 times through our testbed without shaping and collected the resulting tcpdump traces. For each value of ~~ε_W~~ε, we transformed each unshaped trace into a shaped trace using our simulator to generate a total of 4000 shaped traces. We ~~transform the shaped traces and train the classifiers as in §2.1~~also shaped traces for **CR** and **Pacer**.

We train and test BB and TCN on shaped traces as in §2.1 and report the average and standard deviation of the accuracy of each classifier over three runs. Recall from §2.1, the BB and TCN accuracy on unshaped traffic (**Base**) is 0.61 and 0.99, respectively. For **CR** and **Pacer**, the accuracy of both BB and TCN classifiers is 0.025. This is expected since both strategies transform all unshaped traces into a single shape.

Figure 5 shows the ~~average (markers) and the standard deviation (shaded region) of the accuracy of each classifier over three runs on the shaped traces~~classifiers' performance with NetShaper. While BB does not perform well for nearly

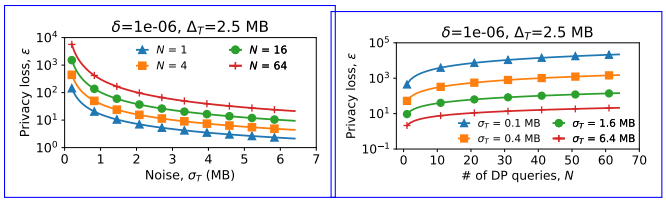

(a) (b)

Figure 6: ~~Per-window privacy loss (ε_W) as a function of (a) noise (σ_T), and (b) number of DP measurements (N).~~ Privacy loss vs (a) noise and (b) # of DP queries.

all values of ~~ε_W~~ε, TCN can be thwarted ~~only for $\varepsilon_W < 1000$. The BB and TCN accuracy on unshaped traffic (~~for ε upto 1000. ~~) is 0.61 and 0.99, respectively (§2.1). In conclusion, while~~ *While even* $\varepsilon \approx 200$ *is too large to offer meaningful theoretical privacy guarantees, it is sufficient to defeat SOTA attacks.*

5.2 Impact of Privacy Parameters

We now evaluate how ~~ε_W varies with~~ ε varies with Δ_T, σ_T, and N~~, and Δ_W~~. Due to space constraints, we present plots for a fixed value of ~~$\Delta_W = 1MB$ and defer additional plots for different values of Δ_W~~ $\Delta_T = 2.5MB$ and defer other plots to §C. ~~We analyze the impact of W and T on latency overheads separately.~~ All analyses use ~~$\delta_W = 10^{-6}$~~$\delta = 10^{-6}$.

Figure 6a shows the ~~trade-off between privacy loss (ε_W) and noise (~~tradeoff between ε and σ_T ~~)~~ over four different ~~numbers of DP measurements (~~values of N~~)~~. Intuitively, a larger σ_T implies higher bandwidth overhead due to DP shaping. To retain a total privacy loss ~~$\varepsilon_W = 1$~~ $\varepsilon = 1$ with at most 4 DP ~~measurements~~queries, we need to add noise with ~~$\sigma_T = 6MB$~~ $\sigma_T = 18MB$ for each DP ~~measurement~~query. In contrast, ~~$\varepsilon_W = 100$~~ $\varepsilon = 200$ with 4 DP ~~measurements~~ queries (approx. configuration that defeats the classifiers in §5.1) only requires ~~$\sigma_T < 0.1MB$. We discuss how to amortize bandwidth overheads using concurrent flows without increasing privacy loss in §5.4 and §5.5.~~

$\sigma_T < 0.3MB$. Figure 6b shows that the total privacy loss escalates with an increase in the number of DP ~~measurements~~queries. While fewer ~~measurements~~ queries within a window (thus larger decision intervals) help to lower the total privacy loss, the ~~trade-off~~ tradeoff is the higher latency overhead~~, which we discuss in~~. We discuss this tradeoff, as well as reduction in bandwidth overheads with concurrent flows in §5.4 and §5.5.

Using these plots, an application can choose suitable values of ~~Δ_W and~~ W and Δ_T to determine the ~~trade-off between ε_W and δ_W~~tradeoff between ε and σ_T. For our web application serving static HTML, we recommend $W = 1s$, since web page downloads in our AWS setup (§2.1) finished within 1s,

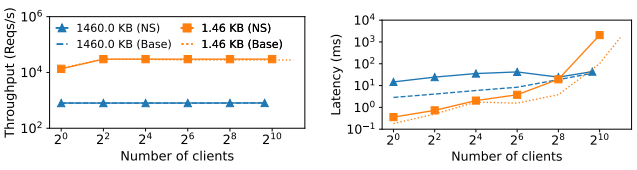

(a) # clients vs throughput (b) # clients vs latency

Figure 7: Throughput and latency overhead due to middleboxes without shaping.

and ~~$\Delta_W = 150KB$~~$\Delta_T = 60KB$, which covers ~~95% of the web pages in our dataset~~all distances. §5.1 explained the choices for our video application. Using ε and T, we can further determine the aggregate privacy loss over longer traffic streams using Rényi-DP composition. For instance, with $\varepsilon = 1$, $W = 5s$, and $T = 1s$, the total privacy loss for a 5 min video, which generates 300 DP queries at 1s intervals, is 8.92; the total loss for a 1 hr video is 38.8. We emphasize that ~~Δ_W and ε_W~~ Δ_T *and* ε *should be selected using ~~trade-off plots similar to Figure 6 and~~ plots like Figure 6, independently of the application's dataset.*

5.3 Performance Microbenchmarks

We now turn our attention to experiments to determine the overheads on per-packet latencies and the peak line rate and throughput sustainable by a NetShaper middlebox.

~~**Middlebox throughput.**~~ **Middlebox throughput.** We measure the peak throughput (requests/s) attained by a server application, the response latency experienced by the clients, and the impact on this throughput and latency due to the middleboxes. We restrict Nginx to one worker thread and one core on the server desktop. We evaluate using two object sizes: 1.4 KB (one MTU) and 1.4 MB. We identify the peak request rate that can be handled by a single wrk2 client, then increase the clients until we find the peak throughput the server can provide. We then vary the number of concurrent clients while generating the peak request load sustainable by the server to find the maximum number of concurrent clients that the server can handle and to measure the impact on the response latency.

We run experiments for 3 min and discard the measurements from the first minute to eliminate startup effects. Figure 7a shows the average of the peak throughput observed across 3 runs. The standard deviation is below 1% in all cases. For 1.4 KB and 1.4 MB objects, the **Base** server achieves a peak throughput of 30K req/s (64 clients) and 800 req/s (800 clients), respectively. $\mathbf{NS_M}$ matches the peak throughput and the max concurrent clients sustained by **Base**.

~~**Latency.**~~ **Latency.** Figure 7b shows the average and standard deviation of the response latencies over a 2 min run. The

ping latency between each pair of directly connected desktops is 0.56 ± 0.18 ms. This overhead comes from the fact that each packet traverses four additional network stacks (across two middleboxes) in each direction. This also involves data copy operations between the kernel and user space. The data copy overhead is proportional to the object size; thus **NS$_M$**'s latency overhead increases with the larger response sizes. ~~The kernel overhead including~~ The kernel data copy overheads are not fundamental to NetShaper's design.

By using kernel bypass techniques or tools like DPDK [31], NetShaper can ~~eliminate data copies between user and kernel space and~~ reduce the latency overhead.

~~**Shaping interval, preparation, and enqueue times.**~~ **Shaping interval, preparation, and enqueue times.** We further profile the middlebox execution to measure the max latencies of the two components in the `Prepare` loop (§4.2): the preparation of the shaped buffer and queuing of the buffer to QUIC worker. These measures determine the maximum durations for preparing and enqueueing shaped buffers (T_{prep} and T_{enq}, respectively), and the minimum value for the shaping interval T. We profile the delays with the middlebox configured with 128 queues. ~~This implies that our middlebox can support~~ , thus supporting a maximum of 128 concurrent clients. One can profile the delays for a different number of queues ~~to support a different number of~~ and concurrent clients.

Based on our measurements, we set $T_{prep} = 6ms$ and $T_{enq} = 1ms$. The smallest value for T that we can configure is 10ms.

~~**Throughput and latency with shaping enabled.**~~ **Throughput and latency with shaping enabled.** We now re-run the microbenchmarks with **NS** configuration. We use three different configurations for T: 10ms, 50ms, and 100ms. We use 128 concurrent clients. The middlebox can sustain the peak throughput of 30K req/s with 1.4KB objects and 700 req/s with 1.4MB objects for each configuration of T. For 1.4KB objects, the average and standard deviation of the response latency with the three configurations are as follows: (i) $T = 10ms$: 30.47 ± 3.89 ms, (ii) $T = 50ms$: 51.39 ± 14.64 ms, (iii) $T = 100ms$: 77.49 ± 28.96 ms. For 1.4MB objects, the latencies are as follows: (i) $T = 10ms$: 41.31 ± 10.84 ms, (ii) $T = 50ms$: 76.96 ± 21.12 ms, (iii) $T = 100ms$: 127.48 ± 45.69 ms. The latency is dominated by the T configuration. The high variance in the latency is due to shaping. If a request arrives just after the decision loop has prepared a buffer in the current iteration, the request will be delayed by at least one iteration of the loop. Moreover, a negative sampling of DP noise may lead to a smaller ~~DP measurement~~ shaped buffer than the available payload bytes in the buffering queues, thus delaying the requests by one or more intervals. This effect is particularly enhanced in a workload close to the line rate. Thus, NetShaper can perform well within about 12-15% of the line rate.

~~**CPU utilization.**~~ **CPU utilization.** The CPU utilization is 3-10% for the `Prepare` core and depends on the DP shaping interval; the utilization is 8-70% for the QUIC worker core, which depends on the network I/O. The `UShaper` core utilizes 100% of the CPU as it polls for packets from `Prepare`. As such, the `Prepare` and QUIC worker cores would be able to support additional tunnel instances by time-sharing their core. By using a polling interval, we could reduce the CPU utilization of `UShaper` to support additional requests at the cost of additional latency. In general, multiple tunnels can time-share the same physical cores, as long as each core runs the same type of thread, to suffice property P4 mentioned in Section 4.2.

5.4 Case Study: Video Streaming

Next, we examine the effect of different privacy settings on bandwidth and latency overheads for video streaming clients.

We run experiments with three values of ~~the DP measurement interval~~ T for the server: 100ms, 500ms, and 1s, and ~~we use $\Delta_W = 1MB$ and $\varepsilon_W = 1$~~max per-flow DP length cutoff of 1.21 MB, 1.22MB, and 1.7 MB, respectively. We use $\Delta_T = 2.5MB$ and $\varepsilon = 1$. For all experiments, we set the DP parameters for client request traffic as follows: ~~$\Delta_W = 200$~~Δ_T = 200 bytes, $W = 1s$, $T = 10ms$, ~~and $\varepsilon_W = 1$~~$\varepsilon = 1$ and max per-flow DP length cutoff of 206 bytes. We run experiments with 1, 16, and 128 video clients; each client requests one video randomly selected from the dataset. For each set of configurations, we measure the average response latency for individual video segments with the testbed as well as the per-flow relative bandwidth overhead for the video streams in the simulator.

~~**Latency and bandwidth overhead.**~~ **Latency and bandwidth overhead.** Figures 8a and 8b respectively show the average segment download latency and the average per-flow relative bandwidth overhead as a function of different intervals and for varying number of clients. The **Base** segment download latency is 2.86 ± 1.41ms. The latency variance is due to variances in the segment sizes. The relative bandwidth overhead of a video is the number of dummy bytes transmitted normalized to the size of the unshaped video stream. The error bars show the standard deviation in latency and bandwidth overhead.

First, Figure 8a shows that, for all values of T, the video segments can be downloaded well within 5s, which is the time to play each segment and request the next segment from the server. The high variance is due to negative DP noise, which delays payload transmission. Secondly, the results show the trade-off between latency and bandwidth. A larger DP ~~measurement~~ interval implies higher download latency but fewer ~~measurements and lower noise added to the~~

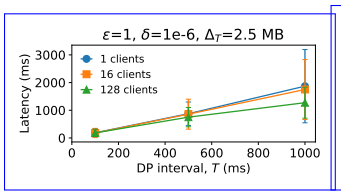

(a) Latency vs DP interval

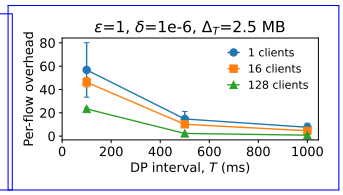

(b) BW overhead vs DP interval

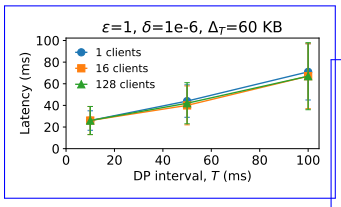

(c) ~~Video streaming.~~ Latency ~~and bandwidth overhead for different values of~~ vs DP interval~~.~~

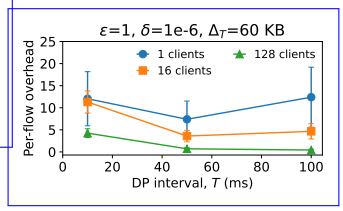

(d) BW overhead vs DP interval

Figure 8: Latency and bandwidth overhead for different values of DP interval for video streaming (a, b) and for web (c, d).

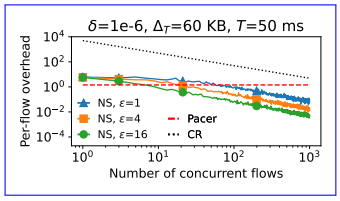

(b) Web service.

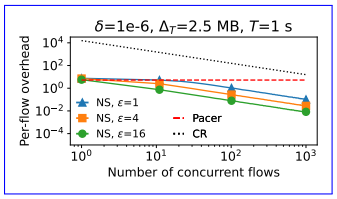

(a) Video streaming.

Figure 9: Comparison of NetShaper, constant shaping, Pacer.

~~payload~~queries, thus yielding a lower bandwidth overhead. Thirdly, with multiple concurrent ~~streaming~~ clients, the bandwidth overhead is amortized, while the average download latency only depends on T. Overall, NetShaper ~~'s shaping~~ can secure video streams with low bandwidth overheads and no impact on the streaming experience.

5.5 Case Study: Web Service

~~Latency vs DP interval BW overhead vs DP interval Web service. Latency and bandwidth overhead for different values of DP interval.~~ We perform similar experiments as §5.4 with our web service. For the server responses, we use ~~$\Delta_W = 150KB$~~$\Delta_T = 60KB$, $W = 1s$, and ~~$\epsilon_W = 1$~~$\varepsilon = 1$. For T, we use 10ms, 50ms, and 100ms, and per-flow DP length cutoffs of 60.8KB, 60.8KB, and 110.9KB, respectively. For the client requests, we use the same configs as in §5.4. We run 3 min experiments with 1, 16, and 128 wrk2 clients with a total load of 1600 req/s~~for both configurations~~; each client requests random web pages from the dataset. We discard the numbers of the first minute.

~~**Latency and bandwidth overhead.**~~ **Latency and bandwidth overhead.** Figures 8c and 8d respectively show the average response latency and the average per-web page relative bandwidth overhead, across all web page requests. The **Base** latency is 0.225 ± 0.3 ms. (The high variance is due to the time precision in wrk2 being restricted to 1ms.) The web workload is more sporadic than video streaming, thus web page download latencies have higher variance than video segment download latency. The absolute latency overhead for **NS** depends on the choice of T. The relative overhead depends on the underlying network latency, which unlike our testbed, is in the order of 10s to 100s of milliseconds in the Internet. Interestingly, the bandwidth overhead for web traffic first reduces with increasing DP ~~measurement~~ shaping interval from 10ms to 50ms, but then increases again with an interval of 100ms. This is because, for small web pages, the DP interval of 100ms is larger than the total time required to download web pages. As a result, additional overhead is incurred due to the padding of traffic in the 100ms intervals.

5.6 Comparison with other techniques

~~Video streaming. Web service. Relative bandwidth overheads of NetShaper(), constant shaping (), and Pacer.~~

Figures 9a and 9b show the per-flow relative bandwidth overhead of **NS**, **CR**, and **Pacer** for video and web applications, respectively, for varying ~~with~~ number of concurrent flows~~and for different values of ϵ_W. We also compare with the overheads that would be incurred due to constant rate shaping () and Pacer , a SOTA system that provides dynamic shaping on a per-client request basis.~~.

For ~~, we configure the peak load for video service corresponding to transmitting 1.7MB in every 5s, and the peak load for web service corresponding to transmitting 57KB every 50ms. These rates correspond to transmitting at a rate that covers the largest object sizes in our video and web datasets.~~

~~In Pacer, for video service, we pad a segment at i^{th} index in a video stream to the largest segment size at that index across all videos in the dataset. For web service, we pad all web pages to the largest page size, i.e., 147KB in our dataset.~~

~~For~~ both video and web traffic, **NS** incurs three orders of magnitude lower overhead than **CR**, which requires continuously transmitting traffic at the peak server load (configured for 1000 clients).

For video traffic, while **NS** incurs similar overhead as Pacer for a single flow with ~~$\epsilon_W = 1$~~$\varepsilon = 1$, it can further amortize

its overheads among multiple concurrent streams within the tunnel without compromising privacy. For web traffic, **NS** requires more than 40 flows to achieve lower overhead than Pacer. Pacer shapes server traffic only upon receiving a client request and does not shape client traffic. Thus, it leaks the timing and shape of client requests, which could potentially reveal information about the server responses [20]. NetShaper shapes traffic in both directions, which incurs higher overhead at the cost of stronger privacy than Pacer.

~~**Evaluation summary.**~~ **Evaluation summary.** Our evaluation provides four insights. (i) There is a huge gap between the theoretical DP guarantees and the privacy configurations required to defeat SOTA attacks. (ii) The latency overhead is dominated by the choice of DP shaping interval, (iii) NetShaper's middlebox can match about 88% of the 10Gbps NIC line rate; a single core of `UShaper` can match the peak throughput of a single core server, (iv) NetShaper's cost is in the two additional cores for `Prepare` and QUIC worker, which helps to avoid any secret-dependent interference in shaping and keep low DP shaping loop lengths. By optimising the implementation, we could use a single middlebox to support larger workloads.

6 Related Work

~~We discuss prior work along three axes: shaping strategy, system architecture, and threat model and goals.~~

~~**Traffic shaping for web.**~~ ~~Prior work has~~ **Traffic shaping for web.** Prior work used traffic shaping~~strategies~~ for defending against website fingerprinting attacks. ~~These strategies can be classified into two types: static and dynamic.~~ Walkie-Talkie [75], Supersequence [74], and Glove [55] use clustering techniques to group objects of a corpus and then shape the traffic of all objects within each cluster to conform to a similar pattern. Traffic morphing [79] makes the traffic of one page look like that of another. These techniques compute traffic shapes that envelope or resemble the network traces of individual objects. ~~Therefore~~Hence, they require a large number of traces to account for ~~variations in traffic shapes due to dynamic network conditions. In contrast,~~ network variations. NetShaper ~~is computationally less expensive because it~~ dynamically adapts traffic shapes based on the prevailing network conditions.

Cs-BuFLO [17], Tamaraw [18], and DynaFlow [47]~~are dynamic techniques that~~, determine traffic shape directly at runtime. ~~Tamaraw, Cs-BuFLO, and DynaFlow~~ They pad object sizes to values that are correlated with the original object sizes, such as the next multiple or power of a configurable constant. ~~The constants determine the padding overhead.~~ These defenses provide privacy akin to k-anonymity, ~~which Tamarawformalizes~~ but have no control on the the size of the anonymous cluster. Tamaraw [18] formalizes the privacy guarantees. NetShaper's DP guarantees are strictly stronger than Tamaraw's (proof in §D).

Differential privacy over streams. Dwork et al. [26] study DP on streams, in which neighboring streams differ in at most one element and the query counts over the stream prefix (without forgetting old information) under a fixed DP budget for the entire stream. NetShaper requires a stronger neighboring definition to model application data streams (Def. 1), but is able to forget the past by dropping stale data from our queue (Assumption 1) and compose privacy loss over time.

NetShaper's neighboring definition is closer to that of user-level DP over streams in [27]. Instead of counting discrete change, however, we use the L1 distance which enables coarsening. Pan-privacy considers an adversary that can compromise the internals of the algorithms (e.g., our buffering queue). This makes the design of algorithms challenging and costly. Instead, we consider the buffering queue private and focus on practical algorithms to study the privacy/overheads trade-off.

~~**Traffic shaping for videos.**~~ Kellaris et al. [42] introduce a notion of DP, called w-event privacy, for streams of length w. Neighboring stream pairs are those whose individual events are pairwise neighbors within a window of upto w. NetShaper's neighboring definition accounts for the maximum stream distance over *any* window of length W, which is a better match for the streams we consider.

Zhang et al. [82] generate differentially private shapes for video streams using ~~the~~ Fourier Perturbation Algorithm (FPA) [58]. FPA transforms ~~an input trace, which is~~ a finite time series of bursts, into a series of DP shaped bursts of the same length. ~~Consequently, FPA cannot guarantee transmission of the entire input byte~~ FPA requires the entire stream's profile upfront, and cannot guarantee complete transmission of an input stream within the shaped trace. ~~Unlike FPA,~~ NetShaper~~dynamically determines DP burst lengths for each transmit interval~~'s DP guarantees simply compose over burst interval sequences, thus allowing shaping of streams of arbitrary lengths with quantifiable privacy and overheads.

Adversarial defenses. Adversarial defenses [6, 33, 38, 54, 57, 62] generate targeted and low-overhead noise to defeat specific classifiers. NetShaper provides provable and configurable privacy against both SOTA as well as future classifiers.

~~**Pacer.**~~ **Network side-channel mitigation systems.** NetShaper's shaping tunnel is conceptually similar to Pacer's [49] cloaked tunnel. However, ~~they have different threat models. Pacer~~ Pacer mitigates leaks of a Cloud tenant's secrets to a colocated adversary through contention at shared network links. Pacer's cloaked tunnel controls the transmit time of TCP packets in accordance with the shaping schedule and congestion control signals. Thus, Pacer ~~'s tunnel endpoint~~ requires non-trivial changes to the network stack on the end

hosts. NetShaper ~~focuses on applications~~ protects applications that are behind private networks ~~that~~ but communicate using the public Internet. ~~Hence, we can place~~ NetShaper's tunnel endpoints can be placed at the interface of the private-public networks, e.g., in a middlebox, thus supporting multiple applications without modifying end hosts. Moreover, by shaping above the transport layer, NetShaper needs to control only the precise timing for generation of bursts of DP length and not the subsequent ~~packetization and~~ transmission to the network.

~~**Censorship circumvention proxies.** Tor , FTE , Scramblesuit , Skypemorph are censorship circumvention systemsthat~~ Ditto [50] and NetShaper propose shaping traffic at network nodes separate from end hosts. NetShaper proposes a hardware-independent, modular and portable middlebox architecture that can be integrated with end hosts, routers, gateways, or even programmable switches as in Ditto.

Censorship circumvention proxies. Censorship circumvention systems [11, 12, 30, 52, 59, 68, 78] rely on traffic obfuscation, scrambling, and transformations of a sensitive application's shape to that of a non-sensitive application. These techniques prevent identification of original protocols by deep packet inspection. ~~But, unlike NetShaper,~~ Unlike NetShaper, they do not prevent inference of secrets from traffic shapes.

~~**Metadata private communication.**~~ **Anonymous communication.** Karaoke [44] and Vuvuzela [70] ~~use constant traffic shaping among participants, but use differential privacy~~ are anonymous messaging systems that use DP to hide participants in a ~~message conversation.~~ conversation, but use constant-rate traffic among the participants. AnoA [9] is a framework to analyze anonymity properties of anonymous communication protocols. AnoA supports DP based quantification for various properties, such as sender anonymity and sender unlinkability. NetShaper~~is different because it provides differentially private traffic shaping to hide~~ 's differentially-private traffic shaping hides the traffic content. In principle, ~~it is possible to combine~~ NetShaper ~~'s DP traffic shaping within a DP message-passing~~ could be combined with an anonymous communication system to provide both content privacy and anonymity ~~.~~ with DP.

7 Conclusion

NetShaper is a provably secure network side-channel mitigation system that provides quantifiable and tunable privacy guarantees in traffic shaping. We believe that NetShaper can eliminate the arms race in network side-channel attacks and defenses and can provide a portable and configurable framework for deploying mitigations for applications with diverse traffic characteristics and in different settings. NetShaper's ~~differential privacy~~ DP based traffic shaping strategy as well as its modular and portable tunnel design can be extended to mitigate leaks in multi-node systems, but we leave the details to future work.

References

[1] A Highw Assurance Cryptographic Library. https://hacl-star.github.io/. Last accessed on 20 Sep 2023.

[2] libsecp256k1. https://github.com/bitcoin-core/secp256k1. Last accessed on 20 Sep 2023.

[3] Pluggable Transports. https://obfuscation.github.io/. Last accessed on 6 Jun 2023.

[4] What is TCP Meltdown? https://openvpn.net/faq/what-is-tcp-meltdown/. Accessed on Apr 30, 2023.

[5] wrk2: A constant throughput, correct latency recording variant of wrk. https://github.com/giltene/wrk2.

[6] Ahmed Abusnaina, Rhongho Jang, Aminollah Khormali, DaeHun Nyang, and David Mohaisen. DFD: Adversarial Learning-based Approach to Defend Against Website Fingerprinting. In *IEEE Conference on Computer Communications (INFOCOMM)*, 2020.

[7] José Bacelar Almeida, Manuel Barbosa, Gilles Barthe, François Dupressoir, and Michael Emmi. Verifying Constant-Time Implementations. In *USENIX Security Symposium*, 2016.

[8] Aslan Askarov, Danfeng Zhang, and Andrew C Myers. Predictive black-box mitigation of timing channels. In *ACM Conf. on Computer and Communications Security (CCS)*, 2010.

[9] Michael Backes, Aniket Kate, Praveen Manoharan, Sebastian Meiser, and Esfandiar Mohammadi. Anoa: A framework for analyzing anonymous communication protocols. In *2013 IEEE 26th Computer Security Foundations Symposium*. IEEE, 2013.

[10] Shaojie Bai, J Zico Kolter, and Vladlen Koltun. An Empirical Evaluation of Generic Convolutional and Recurrent Networks for Sequence Modeling. *arXiv:1803.01271*, 2018.

[11] Diogo Barradas, Nuno Santos, Luís Rodrigues, and Vítor Nunes. Poking a hole in the wall: Efficient censorship-resistant internet communications by parasitizing on webrtc. In *ACM SIGSAC Conference on Computer and Communications Security (CCS)*, 2020.

[12] Diogo Barradas, Nuno Santos, and Luís ET Rodrigues. Deltashaper: Enabling unobservable censorship-resistant tcp tunneling over videoconferencing streams. *Proc. Priv. Enhancing Technol.*, 2017(4):5–22, 2017.

[13] Andrew Beams, Sampath Kannan, and Sebastian Angel. Packet scheduling with optional client privacy. In *ACM Conf. on Computer and Communications Security (CCS)*, 2021.

[14] Matthias Beckerle, Jonathan Magnusson, and Tobias Pulls. Splitting Hairs and Network Traces: Improved Attacks Against Traffic Splitting as a Website Fingerprinting Defense. In *Workshop on Privacy in the Electronic Society (WPES)*, 2022.

[15] Sanjit Bhat, David Lu, Albert Kwon, and Srinivas Devadas. Var-cnn: A data-efficient website fingerprinting attack based on deep learning. In *Privacy Enhancing Technologies Symposium (PETS)*, 2019.

[16] Benjamin A Braun, Suman Jana, and Dan Boneh. Robust and efficient elimination of cache and timing side channels. *arXiv preprint arXiv:1506.00189*, 2015.

[17] Xiang Cai, Rishab Nithyanand, and Rob Johnson. CS-BuFLO: A Congestion Sensitive Website Fingerprinting Defense. In *Workshop on Privacy in the Electronic Society (WPES)*, 2014.

[18] Xiang Cai, Rishab Nithyanand, Tao Wang, Rob Johnson, and Ian Goldberg. A systematic approach to developing and evaluating website fingerprinting defenses. In *ACM SIGSAC Conference on Computer and Communications Security (CCS)*, 2014.

[19] Konstantinos Chatzikokolakis, Miguel E Andrés, Nicolás Emilio Bordenabe, and Catuscia Palamidessi. Broadening the Scope of Differential Privacy Using Metrics. In *Privacy Enhancing Technologies Symposium (PETS)*, 2013.

[20] Shuo Chen, Rui Wang, XiaoFeng Wang, and Kehuan Zhang. Side-Channel Leaks in Web Applications: A Reality Today, a Challenge Tomorrow. In *IEEE Symposium on Security and Privacy (SP)*, 2010.

[21] Giovanni Cherubin, Jamie Hayes, and Marc Juarez. Website Fingerprinting Defenses at the Application Layer. In *Privacy Enhancing Technologies Symposium (PETS)*, 2017.

[22] Bart Coppens, Ingrid Verbauwhede, Koen De Bosschere, and Bjorn De Sutter. Practical Mitigations for Timing-Based Side-Channel Attacks on Modern x86 Processors. In *IEEE Symposium on Security and Privacy (S&P)*, 2009.

[23] George Danezis. Traffic Analysis of the HTTP Protocol over TLS. http://www0.cs.ucl.ac.uk/staff/G.Danezis/papers/TLSanon.pdf, 2009.

[24] Wladimir De la Cadena, Asya Mitseva, Jens Hiller, Jan Pennekamp, Sebastian Reuter, Julian Filter, Thomas Engel, Klaus Wehrle, and Andriy Panchenko. TrafficSliver: Fighting Website Fingerprinting Attacks with Traffic Splitting. In *ACM SIGSAC Conference on Computer and Communications Security (CCS)*, 2020.

[25] Jinshuo Dong, Aaron Roth, and Weijie J Su. Gaussian differential privacy. *Journal of the Royal Statistical Society Series B: Statistical Methodology*, 2022.

[26] Cynthia Dwork, Moni Naor, Toniann Pitassi, and Guy N. Rothblum. Differential Privacy under Continual Observation. In *ACM Symposium on Theory of Computing (STOC)*, 2010.

[27] Cynthia Dwork, Moni Naor, Toniann Pitassi, Guy N Rothblum, and Sergey Yekhanin. Pan-Private Streaming Algorithms. In *International Conference on Supercomputing (ICS)*, 2010.

[28] Cynthia Dwork, Aaron Roth, et al. The Algorithmic Foundations of Differential Privacy. *Foundations and Trends® in Theoretical Computer Science*, 9(3–4):211–407, 2014.

[29] Kevin P Dyer, Scott E Coull, Thomas Ristenpart, and Thomas Shrimpton. Peek-a-boo, I still see you: Why efficient traffic analysis countermeasures fail. In *IEEE Symposium on Security and Privacy (SP)*, 2012.

[30] Kevin P Dyer, Scott E Coull, Thomas Ristenpart, and Thomas Shrimpton. Protocol misidentification made easy with format-transforming encryption. In *ACM Conf. on Computer and Communications Security (CCS)*, 2013.

[31] Linux Foundation. Data plane development kit (DPDK), 2015.

[32] Jiajun Gong and Tao Wang. Zero-delay Lightweight Defenses against Website Fingerprinting. In *USENIX Security Symposium*, 2020.

[33] Jiajun Gong, Wuqi Zhang, Charles Zhang, and Tao Wang. Surakav: Generating Realistic Traces for a Strong Website Fingerprinting Defense. In *IEEE Symposium on Security and Privacy (S&P)*, 2022.

[34] Jamie Hayes and George Danezis. k-fingerprinting: A Robust Scalable Website Fingerprinting Technique. In *USENIX Security Symposium*, 2016.

[35] Andrew Hintz. Fingerprinting websites using traffic analysis. In *Privacy Enhancing Technologies Symposium (PETS)*, 2002.

[36] Nguyen Phong Hoang, Arian Akhavan Niaki, Phillipa Gill, and Michalis Polychronakis. Domain Name Encryption is Not Enough: Privacy Leakage via IP-based Website Fingerprinting. *Privacy Enhancing Technologies Symposium (PETS)*, 2021.

[37] Osamu Honda, Hiroyuki Ohsaki, Makoto Imase, Mika Ishizuka, and Junichi Murayama. Understanding TCP over TCP: effects of TCP tunneling on end-to-end throughput and latency. In *Performance, Quality of Service, and Control of Next-Generation Communication and Sensor Networks III*, volume 6011, pages 138–146, 2005.

[38] Chengshang Hou, Gaopeng Gou, Junzheng Shi, Peipei Fu, and Gang Xiong. Wf-gan: Fighting back against website fingerprinting attack using adversarial learning. In *2020 IEEE Symposium on Computers and Communications (ISCC)*, 2020.

[39] Jana Iyengar and Martin Thomson. QUIC: A UDP-Based Multiplexed and Secure Transport. RFC 9000, May 2021.

[40] Marc Juarez, Mohsen Imani, Mike Perry, Claudia Diaz, and Matthew Wright. Toward an Efficient Website Fingerprinting Defense. In *European Symposium on Research in Computer Security (ESORICS)*, 2016.

[41] Shiva P Kasiviswanathan and Adam Smith. On the 'semantics' of differential privacy: A bayesian formulation. *Journal of Privacy and Confidentiality*, 2014.

[42] Georgios Kellaris, Stavros Papadopoulos, Xiaokui Xiao, and Dimitris Papadias. Differentially private event sequences over infinite streams. *Proceedings of the VLDB Endowment*, 7(12), 2014.

[43] Taesoo Kim, Marcus Peinado, and Gloria Mainar-Ruiz. STEALTHMEM: System-Level Protection Against Cache-Based Side Channel Attacks in the Cloud. In *USENIX Security Symposium*, 2012.

[44] David Lazar, Yossi Gilad, and Nickolai Zeldovich. Karaoke: Distributed private messaging immune to passive traffic analysis. In *USENIX Symposium on Operating Systems Design and Implementation (OSDI)*, 2018.

[45] Mathias Lecuyer, Vaggelis Atlidakis, Roxana Geambasu, Daniel Hsu, and Suman Jana. Certified robustness to adversarial examples with differential privacy. In *IEEE Symposium on Security and Privacy (SP)*, 2019.

[46] Fangfei Liu, Qian Ge, Yuval Yarom, Frank Mckeen, Carlos Rozas, Gernot Heiser, and Ruby B Lee. CATalyst: Defeating last-level cache side channel attacks in cloud computing. In *IEEE International Symposium on High Performance Computer Architecture (HPCA)*, 2016.

[47] David Lu, Sanjit Bhat, Albert Kwon, and Srinivas Devadas. DynaFlow: An Efficient Website Fingerprinting Defense Based on Dynamically-Adjusting Flows. In *Workshop on Privacy in the Electronic Society (WPES)*, 2018.

[48] Xiapu Luo, Peng Zhou, Edmond WW Chan, Wenke Lee, Rocky KC Chang, and Roberto Perdisci. HTTPOS: Sealing Information Leaks with Browser-side Obfuscation of Encrypted Flows. In *Network and Distributed System Security Symposium (NDSS)*, volume 11, 2011.

[49] Aastha Mehta, Mohamed Alzayat, Roberta De Viti, Björn B Brandenburg, Peter Druschel, and Deepak Garg. Pacer: Comprehensive Network {Side-Channel} Mitigation in the Cloud. In *USENIX Security Symposium*, 2022.

[50] Roland Meier, Vincent Lenders, and Laurent Vanbever. Ditto: WAN traffic obfuscation at line rate. In *Network and Distributed System Security Symposium (NDSS)*, 2022.

[51] Ilya Mironov. Rényi differential privacy. In *2017 IEEE 30th computer security foundations symposium (CSF)*, pages 263–275. IEEE, 2017.

[52] Hooman Mohajeri Moghaddam, Baiyu Li, Mohammad Derakhshani, and Ian Goldberg. Skypemorph: Protocol Obfuscation for Tor Bridges. In *ACM Conf. on Computer and Communications Security (CCS)*, 2012.

[53] Milad Nasr, Alireza Bahramali, and Amir Houmansadr. Defeating DNN-Based Traffic Analysis Systems in Real-Time With Blind Adversarial Perturbations. In *USENIX Security Symposium*, 2021.

[54] Milad Nasr, Alireza Bahramali, and Amir Houmansadr. Defeating DNN-Based Traffic Analysis Systems in Real-Time With Blind Adversarial Perturbations. In *USENIX Security Symposium*, 2021.

[55] Rishab Nithyanand, Xiang Cai, and Rob Johnson. Glove: A Bespoke Website Fingerprinting Defense. In *Workshop on Privacy in the Electronic Society (WPES)*, 2014.

[56] Dan Page. Partitioned cache architecture as a side-channel defence mechanism, 2005.

[57] Mohammad Saidur Rahman, Mohsen Imani, Nate Mathews, and Matthew Wright. Mockingbird: Defending Against Deep-Learning-Based Website Fingerprinting

Attacks with Adversarial Traces. *IEEE Transactions on Information Forensics and Security*, 16:1594–1609, 2020.

[58] Vibhor Rastogi and Suman Nath. Differentially private aggregation of distributed time-series with transformation and encryption. In *Proceedings of the 2010 ACM SIGMOD International Conference on Management of data*, pages 735–746, 2010.

[59] Marc B Rosen, James Parker, and Alex J Malozemoff. Balboa: Bobbing and weaving around network censorship. In *USENIX Security Symposium*, 2021.

[60] T Scott Saponas, Jonathan Lester, Carl Hartung, Sameer Agarwal, Tadayoshi Kohno, et al. Devices That Tell on You: Privacy Trends in Consumer Ubiquitous Computing. In *USENIX Security Symposium*, 2007.

[61] Roei Schuster, Vitaly Shmatikov, and Eran Tromer. Beauty and the Burst: Remote Identification of Encrypted Video Streams. In *USENIX Security Symposium*, 2017.

[62] Shawn Shan, Arjun Nitin Bhagoji, Haitao Zheng, and Ben Y Zhao. Patch-based Defenses against Web Fingerprinting Attacks. In *ACM Workshop on Artificial Intelligence and Security (AISec)*, 2021.

[63] Tal Shapira and Yuval Shavitt. Flowpic: Encrypted internet traffic classification is as easy as image recognition. In *IEEE INFOCOM-IEEE Conference on Computer Communications Workshops*, 2019.

[64] Jicheng Shi, Xiang Song, Haibo Chen, and Binyu Zang. Limiting cache-based side-channel in multi-tenant cloud using dynamic page coloring. In *IEEE/IFIP Intl. Conf. on Dependable Systems and Networks Workshops (DSN-W)*, 2011.

[65] Payap Sirinam, Mohsen Imani, Marc Juarez, and Matthew Wright. Deep fingerprinting: Undermining website fingerprinting defenses with deep learning. In *ACM SIGSAC Conference on Computer and Communications Security (CCS)*, 2018.

[66] Jean-Pierre Smith, Luca Dolfi, Prateek Mittal, and Adrian Perrig. QCSD: A QUIC Client-Side Website-Fingerprinting Defence Framework. In *USENIX Security Symposium*, 2022.

[67] Statista. Length of online videos watched on social media platforms worldwide in August 2021, by age group. https://tinyurl.com/9u4ystpe, 2023. Last accessed on 20 Sep 2023.

[68] Paul Syverson, Roger Dingledine, and Nick Mathewson. Tor: The Second-Generation Onion Router. In *Usenix Security*, 2004.

[69] Gang Tan. Principles and Implementation Techniques of Software-Based Fault Isolation. *Foundations and Trends® in Privacy and Security*, 1(3):137–198, 2017.

[70] Jelle Van Den Hooff, David Lazar, Matei Zaharia, and Nickolai Zeldovich. Vuvuzela: Scalable private messaging resistant to traffic analysis. In *Symposium on Operating Systems Principles (SOSP)*, 2015.

[71] Venkatanathan Varadarajan, Thomas Ristenpart, and Michael M Swift. Scheduler-based Defenses against Cross-VM Side-channels. In *USENIX Security Symposium*, 2014.

[72] Bhanu Chandra Vattikonda, George Porter, Amin Vahdat, and Alex C Snoeren. Practical TDMA for Datacenter Ethernet. In *ACM European Conference on Computer Systems (EuroSys)*, 2012.

[73] Mona Wang, Anunay Kulshrestha, Liang Wang, and Prateek Mittal. Leveraging strategic connection migration-powered traffic splitting for privacy. In *Privacy Enhancing Technologies*, 2022.

[74] Tao Wang, Xiang Cai, Rishab Nithyanand, Rob Johnson, and Ian Goldberg. Effective Attacks and Provable Defenses for Website Fingerprinting. In *USENIX Security Symposium*, 2014.

[75] Tao Wang and Ian Goldberg. Walkie-Talkie: An Efficient Defense Against Passive Website Fingerprinting Attacks. In *USENIX Security Symposium*, 2017.

[76] Cedric Westphal, Stefan Lederer, Christopher Mueller, Andrea Detti, Daniel Corujo, Jianping Wang, Marie-Jose Montpetit, Niall Murray, Christian Timmerer, Daniel Posch, Aytac Azgin, and Will Liu. RFC 7933: Adaptive Video Streaming over Information-Centric Networking (ICN). https://datatracker.ietf.org/doc/html/rfc3168. Accessed on Apr 30, 2023.

[77] Andrew M White, Austin R Matthews, Kevin Z Snow, and Fabian Monrose. Phonotactic reconstruction of encrypted voip conversations: Hookt on fon-iks. In *IEEE Symposium on Security and Privacy (S&P)*, 2011.

[78] Philipp Winter, Tobias Pulls, and Juergen Fuss. ScrambleSuit: A Polymorphic Network Protocol to Circumvent Censorship. In *ACM Workshop on Privacy in the Electronic Society (WPES)*, 2013.

[79] Charles V. Wright, Scott E. Coull, and Fabian Monrose. Traffic morphing: An efficient defense against statistical traffic analysis. In *Network and Distributed System Security Symposium (NDSS)*, 2009.

[80] Charles V Wright, Fabian Monrose, and Gerald M Masson. On Inferring Application Protocol Behaviors in

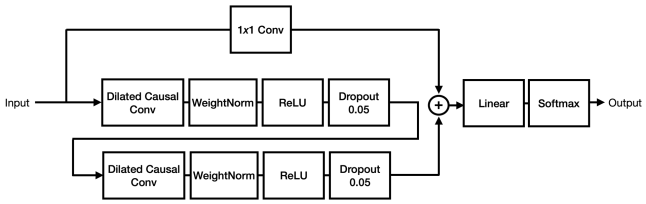

Figure 10: TCN classifier

Encrypted Network Traffic. *Journal of Machine Learning Research (JMLR)*, 7, Dec 2006.

[81] Danfeng Zhang, Aslan Askarov, and Andrew C Myers. Predictive Mitigation of Timing Channels in Interactive Systems. In *ACM Conf. on Computer and Communications Security (CCS)*, 2011.

[82] Xiaokuan Zhang, Jihun Hamm, Michael K Reiter, and Yinqian Zhang. Statistical Privacy for Streaming Traffic. In *ISOC Network and Distributed System Security Symposium (NDSS)*, 2019.

A Attack classifiers

~~**Beauty and Burst.**~~ **Beauty and Burst.** The Beauty and the Burst classifier (BB) [61] is a CNN (convolutional neural network) consisting of three convolution layers, a max pooling layer, and two dense layers. We use a dropout of 0.5, 0.7, and 0.5 between the hidden layers of the network. We train the classifier with an Adam optimizer, a categorical cross-entropy function, a learning rate of 0.01, with a batch size of 64, and for 1000 epochs.

~~**Temporal Convolution Network**~~ **Temporal Convolution Network.** While CNNs are generally effective in sequence modelling, they look at future samples in a sequence and a very limited history of past samples to decide the output of the current sample. Consequently, they require a large number of traces and long traces for effective training and prediction.

Temporal Convolutional Networks (TCNs) [10] overcome these problems of CNNs by utilizing a one-dimensional fully-convolutional network equipped with causal dilated convolutions, which allow them to examine deep into the past to produce an output for the sequence at any given moment.

Figure 10 shows the architecture of our TCN classifier, which follows the architecture proposed by Bai et al. [10]. It consists of two dilated causal convolutional layers, followed by weight normalization and dropout layers with a dropout probability of 0.05. We train the classifier for 1000 epochs.

B Proof of NetShaper's DP based Shaping

Proposition 3. *NetShaper enforces* $\Delta_T \leq \Delta_W$.

To prove ~~the proposition stated above~~Prop 3, we will first establish the following lemma.

Lemma. *Assume two neighboring traffic streams ~~,~~* S_j *and* S'_j *(*$\|S_j - S'_j\|_1 \leq \Delta_W$*), transmitted through NetShaper. If both streams are reshaped to the same output stream ~~,~~*O*, then by the end of any interval of shaping execution, the length of the buffering queue for ~~the first and second streams~~* S *and* S' *are* Δ_W*-close. In other words~~we have~~:*

$$\forall k \geq 0 : |L_k - L'_k| \leq \Delta_W \tag{4}$$

Proof. NetShaper dequeues data from the buffering queue ~~periodically~~ at intervals of T ~~seconds. Thus, while transmitting a stream~~ . While transmitting S, the ~~length of the buffering queue~~ queue length at the end of k^{th} interval ~~,~~T_k is a function of three variables: ~~The length of the buffering queue~~ (i) The buffering queue length L_{k-1} at the end of ~~$(k-1)^{\text{th}}$ interval, L_{k-1}.~~ T_{k-1}. (ii) The total number of payload bytes that have been dequeued from the buffering queue in the k^{th} interval, R_k. (iii) The number of new payload bytes from the application stream added to the buffering queue since the previous interval, which is the sum of sizes of all packets arriving between $(k-1)^{\text{th}}$ and k^{th} interval, i.e., $\sum_{T_{k-1} \leq t < T_k} P_t^S$. ~~As two streams~~ As S and S' are reshaped to the ~~output stream,~~ same O, the ~~DP burst size for~~ shaped buffer length for the two streams is the same in all intervals (i.e. $\forall k \geq 0 : \tilde{L}_k = \tilde{L}'_k$).

Therefore, the ~~length of the buffering queue~~ buffering queue length after dequeue in ~~the k^{th} interval isgiven by:~~ T_k is:

$$L_k = L_{k-1} + \sum_{T_{k-1} \leq t < T_k} P_t^S - R_k \tag{5}$$

~~Based on Equation 5, the difference between~~ The difference between the queue lengths of ~~two neighboring streams,~~ S_j, S'_j at ~~k^{th} interval~~ T_k is:

$$L_k - L'_k = (L_{k-1} - L'_{k-1}) + \left(\sum_{T_{k-1} \leq t < T_k} P_t^S - \sum_{Tk-1 \leq t < T_k} P_t^{S'}\right) - (R_k - R'_k) \tag{6}$$

We divide the proof into two ~~different~~ steps. First, we show that the dequeue stage of the shaping mechanism does not increase the difference in queue lengths. Secondly, we show that under Assumption 1, the enqueue stage of incoming streams does not increase the difference in queue lengths beyond Δ_W.

~~Suppose~~ Given that S_j and S'_j are reshaped to the same output stream ~~,~~O~~. Thus~~, the sizes of output packets generated in each ~~decision~~ interval T when transmitting either streams is the same. However, the content of the output packets in each stream may differ based on the sizes and timing of the packets in each input stream. ~~For the shaping mechanism, this~~ This implies that the number of payload bytes dequeued from the buffering queue ~~for when transmitting each stream~~ during shaping may not necessarily match when transmitting each stream. Nevertheless, the shaping mechanism always satisfies the following inequality:

$$(L_k - L'_k).(R_k - R'_k) \geq 0 \tag{7}$$

To show why Equation 7 always holds, we consider all the possible scenarios for two queue lengths after k^{th} interval:

(i) $L_k,\ L'_k > 0$: This indicates ~~that there are still some untransmitted payload bytes remaining~~ some unsent payload bytes in the buffering queue for both streams~~. Consequently, it~~, which implies that the shaping ~~mechanism~~ does not add any dummy bytes to compensate for the difference between the ~~DP burst size~~ shaped buffer length and the amount of data in the queues. We also know that the ~~DP burst size for two streams are~~ shaped buffer length for the two streams is the same ($\tilde{L}_k = \tilde{L}'_k$)~~Therefore:~~. Therefore $R_k = R'_k \rightarrow R_k - R'_k = 0$.

(ii) $L_k,\ L'_k = 0$: This simply implies $L_k - L'_k = 0$

(iii) $L_k = 0,\ L'_k > 0$: The ~~DP burst size~~ shaped buffer length is the same for both queues. Thus, the first queue provided less payload data since it ~~has~~ emptied out. This means ~~:~~ $R_k \leq R'_k$.

(iv) $L'_k = 0,\ L_k > 0$: This is symmetric to the previous case.

Now, using Equation 7, we prove the following:

$$|L_k - L'_k| \leq |L_{k-1} - L'_{k-1}| + \sum_{T_{k-1} \leq t < T_k} |P_t^S - P_t^{S'}|$$

$$|L_k - L'_k| \leq |L_{k-1} - L'_{k-1}| + \sum_{T_{k-1} \leq t < T_k} |P_t^S - P_t^{S'}| \tag{8}$$

Let's consider $(L_k - L'_k) \geq 0$. (The case of $(L'_k - L_k) \geq 0$ is symmetric.) Using ~~Equation (6)~~Equation 6, we get:

$$\begin{aligned}
|L_k - L'_k| &= L_k - L'_k \\
&= (L_{k-1} - L'_{k-1}) + (\sum_{T_{k-1} \leq t < T_k} P_t^S - P_t^{S'}) - (R_k - R'_k) \\
&\leq (L_{k-1} - L'_{k-1}) + (\sum_{T_{k-1} \leq t < T_k} P_t^S - P_t^{S'}) \\
&\leq |(L_{k-1} - L'_{k-1}) + (\sum_{T_{k-1} \leq t < T_k} P_t^S - P_t^{S'})| \\
&\leq |L_{k-1} - L'_{k-1}| + \sum_{T_{k-1} \leq t < T_k} |P_t^S - P_t^{S'}|
\end{aligned}$$

Intuitively, this means the dequeue stage ~~,~~never increases the difference between ~~two queues lengths. Now~~queue lengths. Under Assumption 1, we show ~~that under Assumption 1, the difference in queue lengths~~ the difference is bounded. With $d_k = |L_k - L'_k|$~~and $d_0 = 0$,we have~~, $d_0 = 0$:

$$\begin{aligned}
d_k &\leq d_{k-1} + \sum_{T_{k-1} \leq t < T_k} |P_t^S - P_t^{S'}| \\
&= 0 + \sum_{i=0}^{k} (\sum_{T_{i-1} \leq t < T_i} |P_t^S - P_t^{S'}|) \\
&= \sum_{0 \leq t < T_k} |P_t^S - P_t^{S'}| \\
&= \sum_{0 \leq t < T_k - W} |P_t^S - P_t^{S'}| + \sum_{T_k - W \leq t < T_k} |P_t^S - P_t^{S'}| \\
&= 0 + \|S_j - S'_j\|_1 \leq \Delta_W
\end{aligned}$$

□

~~Distribution of the difference in buffering queue lengths for pairs of an application's streams.~~

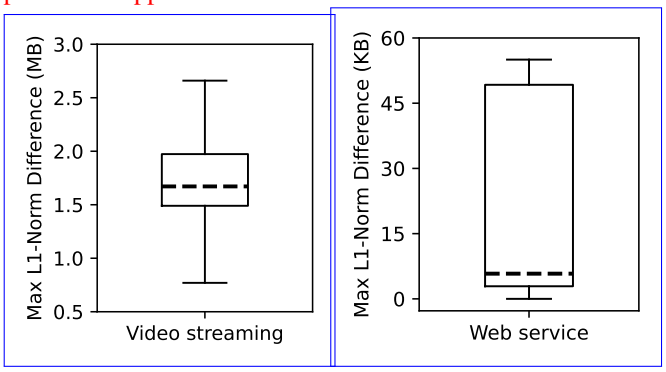

(a) ~~Noise vs privacy loss~~Video streaming (b) ~~Number of DP updates vs privacy loss~~Web service

Figure 11: Distribution of the difference in buffering queue lengths for application stream pairs.

To conclude, the maximum difference between queue lengths (i.e., the sensitivity, Δ_T) is always bounded by Δ_W.

$$\Delta_T = \max_{k=0}^{\lceil \frac{W}{T} \rceil} \max_{S_j, S'_j} |L_k - L'_k| \leq \Delta_W \tag{9}$$

C Extended evaluation of privacy ~~loss~~ vs ~~noise~~ overheads

~~Figure 12 shows the relation between per-window privacy loss (ε_W), noise overhead in MB (σ_W), sensitivity in MB (Δ_W), and number of DP measurements (N) at a lower scale of sensitivity (Δ_W) for two different setups: applications with high sensitivity values (e.g. 10 MB) where the queue size undergoes significant changes across different streams and applications with low sensitivity (e.g. 0.1 MB).~~

~~In addition, the boxplot in Appendix C shows the~~ Figures 11a and 11b show the distribution of the difference in buffering queue lengths generated for each pair of an application's streams. The ~~shaping~~ neighboring window length W is ~~assumed to be~~ 5s for video streams and 1s for web pages. The error bars show the ~~minimum and maximum differences, and~~ min and max differences, the boxes show the first and third quartiles. The dashed lines show the median difference, which is ~~and for video streaming and web service~~1.63 MB and 6 KB for videos and web pages, respectively.

Figure 12 shows similar results as Figure 6 for other Δ_T.

D Comparison of NetShaper and Tamaraw

~~Prior work has proposed several shaping strategies, although many of them use ad hoc heuristics for shaping various features of network traffic to mitigate network side-channel~~

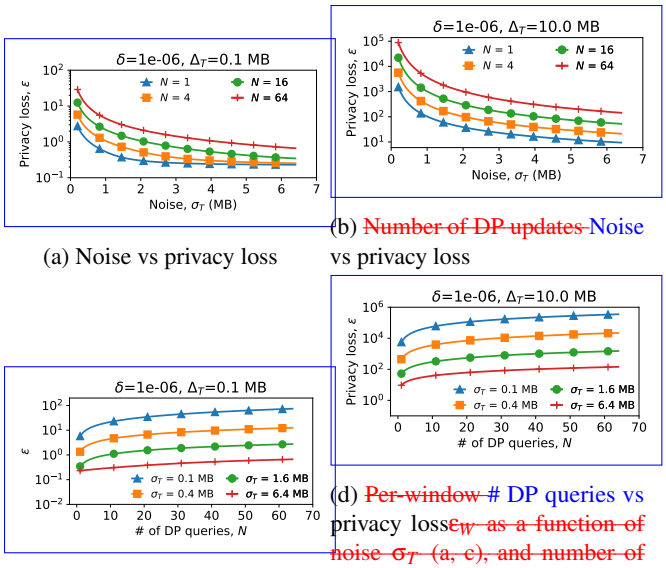

(a) Noise vs privacy loss

(b) ~~Number of DP updates~~ Noise vs privacy loss

(c) # DP queries vs privacy loss

(d) ~~Per-window~~ # DP queries vs privacy loss~~ε_W as a function of noise σ_T (a, c), and number of DP measurements N (b, d).~~

Figure 12: Privacy loss vs noise and # queries for different Δ_T.

~~leaks.~~ Tamaraw [18] provides a mathematical notion of privacy guarantee of a shaping strategy, called ε-security. To disambiguate with NetShaper's notion of ~~$(\varepsilon_W, \delta_W)$~~$(\varepsilon, \delta)$-DP, we rename Tamaraw's ε variable with γ~~in this section.~~

. We show that NetShaper's ~~$(\varepsilon_W, \delta_W)$~~$(\varepsilon, \delta)$-DP definition is strictly stronger than Tamaraw's γ-security definition.

~~We start by explaining~~ First, we explain Tamaraw's ~~definition. Tamaraw defines~~ γ-security definition. In Tamaraw, W ~~as the random variable that represents~~ is a random variable representing the label of a traffic trace. For ~~each traffic trace ,~~ a trace w, ~~let T_w T_w^D be~~ the random variables ~~representing~~ T_w and T_w^D respectively represent the packet trace of w before and after ~~applying shaping on w respectively~~shaping with a defense D. The distribution of T_w^D ~~encompasses~~ captures all variations in ~~observed patterns of a trace~~ the observed shape of w resulting from both the defense mechanism and the network, ~~and~~ while the distribution of T_w only ~~captures the randomness added in the~~ contains variations due to the network. The attacker can measure the distribution of W and T_w^D independently.

Upon observing a network trace t~~on the network~~, an optimal attack A, selects the label ~~that corresponds to the~~ of the trace with maximum likelihood of ~~observing that trace.~~ observation:

$$A(t) = \underset{w}{\operatorname{argmax}} \Pr[W = w] \Pr[T_w^D = t]$$

~~For any attack~~ The probability that an attack A ~~, we represent the probability that attack output the~~ outputs label w_i ~~with~~ is $\Pr_A[w_i]$.

Definition (Tamaraw γ-privacy)**.** *A fingerprinting defense D is said to be uniformly γ-private if for the attack $\mathcal{A}$ if we have:*

$$\max_w \left[\Pr[A(T_w^D) = w]\right] \leq \gamma$$

Proposition 4. *Tamaraw γ-privacy is strictly weaker than the notion of ε-differential privacy. ~~To prove the above proposition, we need to~~*

To prove Prop 4, we prove the following two lemmas.

Lemma 1. *There exists a Tamaraw γ-private defense mechanism that fails to satisfy ~~(ε)-differential privacy~~ ε-DP for any given value of ε.*

Proof. Consider a web service with a dataset of n web pages. We propose ~~the following defense mechanism,~~ a defense D, ~~with two parameters α and β: For the webpage $w_i : i = j$, D reshapes it to the~~ which shapes pages to a constant-rate pattern ~~, O_c , with probability~~ with probabilities α or β. ~~Otherwise, with probability $1-\beta$, it reveals the original traffic pattern of the webpage, $T_{w_{i=j}}$. For any webpage $w_i : i \in \{1, 2, \ldots, j-1, j+1, \ldots, n\}$, D~~ reshapes ~~it to the constant-rate pattern,~~ page w_j to O_c ~~, with probability α such that $\alpha > e^{\varepsilon}\beta$. Otherwise, D reveals the original pattern of w_i, $T_{w_{i\neq j}}$,~~ with probability β and all other pages $w_i \neq w_j$ with probability α. If a page is not shaped, it is revealed.

The probability that any attack can correctly identify the label for ~~webpage~~ w_j is upper-bounded by:

$$\begin{aligned}
&\Pr[A(T^D_{w_{i=j}}) = w_j] \\
&= \Pr[A(T^D_{w_{i=j}}) = w_j | T^D_{w_{i=j}} = T_{w_{i=j}}] \Pr[T^D_{w_{i=j}} = T_{w_{i=j}}] + \\
&\quad \Pr[A(T^D_{w_{i=j}}) = w_j | T^D_{w_{i=j}} = O_c] \Pr[T^D_{w_{i=j}} = O_c] \\
&\leq 1.(1-\beta) + \frac{1}{n}\beta = p_c^j
\end{aligned}$$

For $(1 - \frac{n\gamma-1}{n-1}) < \beta$ we have: $p_c^j \leq \gamma$. Similarly, the probability that any attack can correctly classify $w_{i\neq j}$ is upper-bounded by $p_c^i = 1 - \alpha + \frac{\alpha}{n}$, and for $(1 - \frac{n\gamma-1}{n-1}) < \alpha$ we have: $p_c^j \leq \gamma$. Therefore, for all values of α and β such that $(1 - \frac{n\gamma-1}{n-1}) < \beta < \alpha$, the probability that any attack can successfully guess~~victim traffic stream in both cases~~ a page is less than γ, and the defense is uniformly γ-private.

When the output of the algorithm is ~~a constant pattern,~~ O_c, ~~with the probability β the original webpage is j, and with probability~~ the probability of the page being w_j is β and any other page is α~~, it can be any other webpages~~. Thus, ~~we have:~~

$$\log\left(\frac{\Pr[T^D_{w_{i\neq j}} = O_c]}{\Pr[T^D_{w_{i=j}} = O_c]}\right) = \log\left(\frac{\alpha}{\beta}\right) \geq \varepsilon.$$

~~Therefore, it fails to guarantee~~ By setting $\alpha > e^{\varepsilon}\beta$, we get a mechanism that is γ-private for Tamaraw but not ε-~~differential privacy~~-DP for NetShaper. □

Lemma 2. *A ε-~~differentially private~~ -DP shaping algorithm is Tamaraw γ-private for ~~:~~*

$$\varepsilon \leq \log(n\gamma)$$

$\varepsilon \leq \log(n\gamma)$.

Proof. For a ~~given trace ,~~ trace w, the random variable T_w^{DP} represents the packet trace of w after a differentially private shaping mechanism is applied. The classification attack on shaped traffic ~~analysis the shaped traces so it~~ can be considered ~~as~~ a post-processing of the results of a differentially private shaping mechanism (i.e. defense) ~~, and~~and, hence, is differentially private. Therefore, we have:

$$\frac{\Pr[A(T_{w_i}^{DP}) = w_i]}{\Pr[A(T_{w_j}^{DP}) = w_i]} \leq e^{\varepsilon}$$

$$\rightarrow\Rightarrow \Pr[A(T_{w_i}^{DP}) = w_i] \leq e^{\varepsilon}.\Pr[A(T_{w_j}^{DP}) = w_i]$$

Intuitively, this implies that the likelihood of the attacker correctly classifying the trace with label i compared to incorrectly classifying it with label j is bounded by e^{ε}. The above inequality is correct for all $w_j : j \in \{1,2,\ldots,n\}$, ~~therefore we can~~ and we can extend the above equation to calculate the summation over j~~. Extending the above equation we have:~~ :

$$n \times \Pr[A(T_{w_i}^{DP}) = w_i] \leq e^{\varepsilon} \sum_{j=1}^{n} \Pr[A(T_{w_j}^{DP}) = w_i]$$

$$= e^{\varepsilon} \Pr_A[w_i]$$

~~where $\Pr_A[w_i]$ is the probability that attack A outputs the label w_i. Therefore~~Thus, for any given trace w_i, the probability that any attack A, classifies it correctly is bounded by:

$$\Pr[A(T_{w_i}^{DP}) = w_i] \leq \frac{e^{\varepsilon} \Pr_A[w_i]}{n}$$

~~Therefore, the~~ The probability that an attacker can guess the victim's trace is bounded by:

$$\max_{w_i} \Pr[A(T_{w_i}^{DP}) = w_i] \leq \frac{e^{\varepsilon}}{n} \max_{w_i} \Pr_A[w_i] \leq \frac{e^{\varepsilon}}{n} \leq \gamma$$

□

~~Putting the two lemmas together, we prove that the notion of differential privacy is strictly stronger than Tamaraw's.~~